A Humanized Yeast System for Evaluating the Protein Prenylation of a Wide Range of Human and Viral CaaX Sequences

Emily R. Hildebrandt[1], Anushka Sarkar[1], Rajani Ravishankar[1], June H. Kim[1] and Walter K. Schmidt[1,2]

1. Department of Biochemistry and Molecular Biology, University of Georgia
2. Corresponding Author: Walter K. Schmidt, 706-583-8241 (phone), wschmidt@uga.edu (email), 120 East Green Street, Athens, GA 30602

Running Title

A humanized yeast system for evaluating CaaX protein prenylation

Key words

CaaX, farnesylation, geranylgeranylation

Total Word Count (not including References, Methods or Supplemental): 7967

1 **Summary Statement:** We report yeast engineered to express human prenylation enzymes with

2 which prenylation can be investigated for established and novel CaaX sequences associated with

3 proteins involved in human disease.

4

5 **Abstract (218 words)**

6 The C-terminal CaaX sequence (cysteine-aliphatic-aliphatic-any of several amino acids)

7 is subject to isoprenylation on the conserved cysteine and is estimated to occur in 1-2% of

8 proteins within yeast and human proteomes. Recently, non-canonical CaaX sequences in

9 addition to shorter and longer length CaX and CaaaX sequences have been identified that can be

10 prenylated. Much of the characterization of prenyltransferases has relied on the yeast system

11 because of its genetic tractability and availability of reporter proteins, such as the **a**-factor mating

12 pheromone, Ras GTPase, and Ydj1 Hsp40 chaperone. To compare the properties of yeast and

13 human prenyltransferases, including the recently expanded target specificity of yeast

14 farnesyltransferase, we have developed yeast strains that express human farnesyltransferase or

15 geranylgeranyltransferase-I in lieu of their yeast counterparts. The humanized yeast strains

16 display robust prenyltransferase activity that functionally replaces yeast prenyltransferase

17 activity in a wide array of tests, including the prenylation of a wide variety of canonical and non-

18 canonical human CaaX sequences, virus encoded CaaX sequences, non-canonical length

19 sequences, and heterologously expressed human proteins HRas and DNAJA2. These results

20 reveal highly overlapping substrate specificity for yeast and human farnesyltransferase, and

21 mostly overlapping substrate specificity for GGTase-I. This yeast system is a valuable tool for

22 further defining the prenylome of humans and other organisms, identifying proteins for which

23 prenylation status has not yet been determined.

24 **Introduction**

25 Post-translational modification of the C-terminal CaaX[1] sequence is important for regulating the

26 localization and function of many proteins, including the Ras GTPases often cited as archetypical

---

[1] the term CaaX will refer to all C-terminal tetrapeptide sequences whether or not they fit the traditional consensus sequence.

27   CaaX proteins (Campbell and Philips, 2021; Cox et al., 2015; Ravishankar et al., 2023). CaaX

28   proteins are functionally involved in disease states, such as cancer, Alzheimer's disease and viral

29   infections, including Hepatitis D and SARS-CoV2 (Jeong et al., 2022; Marakasova et al., 2017;

30   Ring et al., 2022; Soveg et al., 2021; Wickenhagen et al., 2021).

31   The C-terminal CaaX sequence has been traditionally defined as a Cysteine (C), two aliphatic

32   amino acids (a_1a_2), and one of several amino acids (X). The first step in CaaX modification is

33   covalent attachment of a farnesyl (C15) or geranylgeranyl (C20) isoprene lipid to the Cysteine.

34   farnesyltransferase (FTase) generally targets CaaX sequences, while geranylgeranyltransferase-I

35   (GGTase-I) targets the subset of CaaL/I/M sequences (Hartman et al., 2005). CaaX sequences

36   with an aliphatic amino acid at the a_2 position commonly follow the canonical modification

37   pathway that involves three steps: initial isoprenylation, proteolytic removal of aaX, and

38   carboxymethylation of the exposed prenylated cysteine. In yeast, the Ras2 GTPase and **a**-factor

39   mating pheromone are highly studied examples of canonically modified CaaX proteins. In

40   addition, CaaX sequences lacking a_1 and a_2 aliphatic residues can be farnesylated (Kim et al.,

41   2023). These so-called shunted CaaX sequences retain their last three amino acids, resulting in a

42   biochemically distinct C-terminus compared to canonically modified CaaX proteins (Hildebrandt

43   et al., 2016b). The yeast Ydj1 HSP40 protein is a recently characterized example of a shunted

44   CaaX protein.

45   Farnesylation and geranylgeranylation of CaaX sequences is accomplished by heterodimeric

46   farnesyltransferase (FTase) and geranylgeranyltransferase-I (GGTase-I), respectively. The

47   enzymes share an α subunit while the β subunits provide isoprenoid specificity and substrate

48   recognition (Lane and Beese, 2006; Maurer-Stroh et al., 2003). Human FTase (*Hs*FTase) is

49   composed of *Hs*FNTA and *Hs*FNTB subunits; the orthologous subunits of yeast *Saccharomyces*

50   *cerevisiae* FTase (*Sc*FTAse) are *Sc*Ram2 and *Sc*Ram1 (**Figure 1A**). Human GGTase-I

51   (*Hs*GGTase-I) is composed of *Hs*FNTA and *Hs*PGGT1B subunits, while the orthologous

52   subunits of yeast GGTase-I (*Sc*GGTase-I) are *Sc*Ram2 and *Sc*Cdc43. In yeast, *RAM1* is not an

53   essential gene (i.e., *ram1Δ* strains are viable), whereas *RAM2* and *CDC43* are essential, raising

54   the possibility that GGTase-I is more critical to yeast life processes relative to FTase.

55   There are 1207 annotated human proteins possessing a CaaX sequence (i.e., Cysteine followed

56   by any 3 amino acids at the C-terminus) within UniProtKB/Swiss-Prot representing 680 unique

57   sequences among the 8000 possible CaaX amino acid combinations. There are also 375 viral

58   proteins possessing a CaaX sequence that could potentially utilize host enzymes for

59   isoprenylation (**Table 1**). Determining the prenylation status of candidate CaaX sequences has

60   depended on a variety of methods and prediction algorithms, each with its own limitations.

61   Methods for case-by-case verification of protein prenylation include radiolabeling with ^{3}H-

62   mevalonate, gel mobility analysis, localization studies and mass spectrometry (Anderegg et al.,

63   1988; Hancock et al., 1989; Hildebrandt et al., 2016b; Michaelson et al., 2005; Ravishankar et

64   al., 2023). Methods for systematic verification have relied on metabolic labeling with reagents

65   compatible with click chemistry, peptide arrays, and genetic approaches (Kho et al., 2004; Kim

66   et al., 2023; Rashidian et al., 2013; Storck et al., 2019; Suazo et al., 2018; Suazo et al., 2021;

67   Wang et al., 2014). Differentiating FTase and GGTase-I target specificity has mostly relied on

68   *in vitro* and genetic approaches (Hougland et al., 2010; Kim et al., 2023; Stein et al., 2015).

69   Independent of the methods employed, it remains a distinct challenge to confirm the predictive

70   prenylation of candidate CaaX sequences, especially across species where conservation of target

71   specificity has not necessarily been confirmed.

72   In this study, we have developed yeast strains expressing *Hs*FTase and *Hs*GGTase-I that

73   functionally replace the yeast prenyltransferases in a wide array of tests. Results with a universal

74   reporter for both farnesylation and geranylgeranylation indicate highly overlapping target

75   specificity across species for each prenyltransferase. We also demonstrate the utility of these

76   strains for testing the in vivo prenylation of heterologously expressed human proteins. These

77   humanized strains provide a valuable new resource for protein prenylation research, especially

78   for target specificity studies of the human prenyltransferase in a genetically amenable cell-based

79   system. This resource is expected to enhance the identification and characterization of novel

80   prenyltransferase targets, including those harboring atypical CaaX sequences.

81   **Results**

82   **Interspecies complementation analysis of FTase subunits**

83 As a key first step toward developing a yeast system to express *Hs*FTase, complementation

84 studies were performed to assess the functional equivalence of yeast and human FTase subunits.

85 Codon optimized genes encoding *Hs*FNTB and *Hs*FNTA were introduced into yeast and

86 evaluated for the ability to complement for loss of yeast FTase β subunit Ram1 (i.e., *ram1Δ)*

87 using an assay that measures production of the farnesylated **a**-factor mating pheromone (**Figure**

88 **1B**). No **a**-factor was produced by *ram1Δ* yeast, while complementation with plasmid-encoded

89 Ram1 restored **a**-factor production to near normal levels as measured using an **a**-factor

90 dependent yeast mating assay (i.e., 0% and 83.6% mating relative to WT, respectively). As

91 expected, plasmid encoded *Hs*FNTA did not complement for activity since this strain only

92 carries copies of FTase α subunits (yeast and human). Many human orthologs of yeast proteins

93 can substitute for their yeast counterpart, yet *Hs*FNTB was unable to do so, implying that either

94 the yeast Ram2 and *Hs*FNTB subunits do not interact or a hybrid FTase complex (Ram2-

95 *Hs*FNTB) is non-functional. In fact, **a**-factor was produced only when the human FTase α and β

96 subunits were co-expressed. The observed mating activity was slightly below wildtype levels

97 when *Hs*FTase subunits were plasmid-encoded (70.8% of WT) and at wildtype levels when

98 subunits were integrated into the genome (100.5% of WT). These phenotypes were derived

99 using the strong constitutive phosphoglycerate kinase promoter (i.e., P_{PGK1}) to drive expression

100 of *Hs*FTase subunits. Expression of *Hs*FNTA and *Hs*FNTB from their orthologous yeast

101 promoters restored mating to less than 1% of wildtype (**Supplemental Figure S1**).

102 To confirm the ability of yeast expressed *Hs*FTase to fully prenylate other CaaX proteins, the

103 extent of endogenous Ydj1 farnesylation was determined by gel-shift analysis (**Figure 1C**).

104 Farnesylated Ydj1 has faster gel mobility than unfarnesylated Ydj1 when analyzed by SDS-

105 PAGE and immunoblot. Using the same strains evaluated for **a**-factor production, farnesylation

106 of Ydj1 was evident only when *Sc*FTase or *Hs*FTase dimeric complex was present.

107 Farnesylation of Ydj1 by *Hs*FTase was qualitatively complete. When combined with the

108 analysis of **a**-factor production, these results indicate that *Hs*FTase activity is unlikely to be

109 limiting at the cellular level. In addition, we confirmed the ability of chromosomally integrated

110 *Hs*FTase to reverse the temperature sensitive growth phenotype of *ram1Δ* yeast (**Figure 1D**).

111 Together, the results of these complementation studies indicate that *Hs*FTase activity can be

112 engineered to mimic the *Sc*FTase activity levels in a cell-based system.

*Hs*FTase expressed in yeast modifies human Ras CaaX sequences

Our complementation studies indicated that *Hs*FTase can modify yeast proteins harboring either a canonical CaaX sequence (**a**-factor; CVIA) or a shunted CaaX sequence (Ydj1; CASQ). To extend this observation to other protein contexts and canonical sequences, the farnesylation of the yeast Ras2 GTPase (*Sc*Ras2) was evaluated using the chromosomally integrated *Hs*FTase yeast strain (**Supplemental Figure S2A**). *Sc*Ras2 has 65.6% and 64.4% identity to human NRas and HRas, respectively. In yeast and humans, Ras localization to the plasma membrane depends on canonical modification of the CaaX sequence (Boyartchuk et al., 1997; Michaelson et al., 2005; Ravishankar et al., 2023). Indeed, GFP-*Sc*Ras2 with its natural CaaX sequence (CIIS) was localized to the plasma membrane when *Sc*FTase or *Hs*FTase was expressed (**Figure 2A**; *Sc* and *Hs*, respectively). GFP-*Sc*Ras2 was mislocalized in the absence of FTase activity (*ram1Δ*) or when harboring a CaaX cysteine to serine substitution mutation (SIIS), as has been previously observed (Dong et al., 2003; Ravishankar et al., 2023).

We utilized the GFP-*Sc*Ras2 reporter to further evaluate the ability of *Hs*FTase to recognize CaaX sequences associated with human Ras orthologs: *Hs*KRas4A (CIIM), *Hs*NRas (CVVM), *Hs*HRas (CVLS), and *Hs*KRas4B (CVIM) (**Figure 2B**). All the sequences directed GFP-*Sc*Ras2 to the plasma membrane, indicating that they are farnesylated by *Hs*FTase. As additional confirmation of prenylation by *Hs*FTase, the mobilities of GFP-*Sc*Ras2-CaaX variants were analyzed by gel-shift assay (**Figure 2C**). Like farnesylated Ydj1, prenylated *Sc*Ras2 migrates faster relative to unprenylated protein when analyzed by SDS-PAGE. GFP-*Sc*Ras2 exhibited faster mobility relative to protein produced in the absence of FTase (i.e., *ram1Δ*) in the context of its wildtype sequence (CIIS) and two human Ras CaaX sequences (CVVM and CVLS; CIIM and CVIM are discussed below), indicative of complete prenylation. Gel-shift studies were also used to examine the farnesylation of heterologously expressed human oncogenic protein Myc-HRas61 (CVLS) that was heterologously expressed in the humanized yeast strain (Adari et al., 1988; Farnsworth et al., 1991). It too was completely prenylated (**Figure 2D**).

Some CaaX sequences, including those associated with KRas4A (CIIM), KRas4B (CVIM) and NRas (CVVM), are alternately prenylated by *Hs*GGTase-I in the absence of *Hs*FTase activity, which is often established in systems through the action of FTase inhibitors (Mohammed et al.,

6

142   2016; Whyte et al., 1997). Consistently, GFP-*Sc*Ras2-CaaX variants harboring CIIM and CVIM

143   sequences exhibited mobility shifts of less magnitude in the gel-shift assay (**Figure 2C**), which

144   we attribute to alternate prenylation by yeast GGTase-I in the absence of FTase (*ram1Δ*). To

145   bolster this conclusion, we determined that GFP-*Sc*Ras2-CaaX variants CIIM and CVIM

146   exhibited plasma membrane localization in the FTase-deficient *ram1Δ* strain, which would be

147   predicted if they were geranylgeranylated (**Figure 2E**). Combined, these observations suggest

148   that *Sc*GGTase-I also has the opportunistic ability to modify certain CaaX sequences in the

149   absence of FTase activity (i.e., *ram1Δ*), resulting in geranylgeranylated products having similar

150   although not identical mobility as the farnesylated products.

_Hs_FTase expressed in yeast modifies the non-canonical human DNAJA2 CAHQ sequence

152   The ability of *Sc*FTase to modify the non-canonical CaaX sequence associated with Ydj1

153   (CASQ) and other non-canonical sequences has been reported (Berger et al., 2018; Hildebrandt

154   et al., 2016b; Kim et al., 2023; Ravishankar et al., 2023). The complementation studies described

155   above indicate that *Hs*FTase can also modify the Ydj1 CASQ sequence (see **Figure 1**). To

156   further investigate the breadth of sequences recognized by *Hs*FTase, we used thermotolerance

157   and gel-shift assays to evaluate a set of Ydj1-CaaX variants representing sequences that are well

158   characterized in terms of modification status. In the thermotolerance assay, yeast lacking Ydj1

159   (vector) or an unmodifiable Ydj1(SASQ) are unable to grow at 40 °C because Ydj1 farnesylation

160   is required for efficient growth at elevated temperatures (**Figure 3A**). All the remaining Ydj1-

161   CaaX variants exhibited growth profiles that were nearly identical whether farnesylation was

162   supported by *Sc*FTase or *Hs*FTase. Yeast expressing Ydj1 with prenylation-only sequences

163   (CASQ and CAHQ) supported the most robust thermotolerance; these sequences were derived

164   from yeast Ydj1 and human DNAJA2, respectively. The prenylation-only status of CAHQ was

165   previously based on homology and prediction algorithms (Hildebrandt et al., 2016b; Kim et al.,

166   2023) and is confirmed here by the observation that CAHQ supports thermotolerance similar to

167   CASQ and is resistant to proteolysis by the CaaX proteases (**Supplemental Figure S3**). Yeast

168   expressing Ydj1 with canonical CaaX sequences (CVIA and CTLM) exhibited partial growth

169   under this condition as has been previously observed (Hildebrandt et al., 2016b); these sequences

170   were derived from yeast **a**-factor and Gγ Ste18, respectively. Side-by-side SDS-PAGE analysis

171   of the Ydj1-CaaX variants revealed that both canonical and prenylation-only CaaX sequences are

7

172   fully prenylated by both *Sc*FTase and *Hs*FTase (**Figure 3B**). Additional support for the ability of

173   *Hs*FTase to modify these sequences is evident when comparing the mobilities of Ydj1-CaaX

174   variants in the absence of FTase (i.e., *ram1Δ*) (**Figure 3C**).

175   The observations made using Ydj1 as a reporter were also evident for *Hs*DNAJA2 (CAHQ) that

176   was heterologously expressed in the humanized yeast strain. *Hs*DNAJA2 has 46% identity to

177   Ydj1 and can complement some Ydj1-associated defects (Whitmore et al., 2020). *Hs*DNAJA2

178   supported thermotolerance in the context of both *Sc*FTase and *Hs*FTase strains, and this

179   phenotype was prenylation dependent because DNAJA2-SAHQ did not support thermotolerance

180   (**Figure 3D**). By gel-shift analysis, both *Sc*FTase and *Hs*FTase modified *Hs*DNAJA2 (**Figure**

181   **3E**). These results further extend the utility of the humanized yeast strain for studies of

182   heterologously expressed human CaaX proteins. Moreover, these observations support the

183   hypothesis that *Sc*FTase and *Hs*FTase have highly similar sequence recognition profiles that are

184   likely broader than the CaaX consensus sequence.

185   **_Hs_FTase expressed in yeast modifies a range of human and viral CaaX protein sequences**

186   Studies on the prenylation of CaaX proteins in most systems is hindered by several factors

187   ranging from difficulty in odetection of low abundance proteins, to lack of phenotypic readouts,

188   to labor and time costs for case-by-case studies. Many of these hurdles can be overcome using

189   the Ydj1 reporter and genetically tractable yeast system described in this study. To support the

190   utility of our approach for investigations of *Hs*FTase specificity, Ydj1-CaaX variants harboring

191   the CaaX sequences of known prenylated human proteins were evaluated by gel-shift assay.

192   Each variant was evaluated in the presence and absence of *Hs*FTase to ensure that gel-shifts were

193   due to *Hs*FTase and to assess whether alternate prenylation was possible. The CaaX sequences

194   evaluated were from chaperone proteins (Nap1L1, DNAJA1 and Pex19), chromosome stability

195   proteins (CENPE, CENPF and Spindly), nuclear lamins (Prelamin A and Lamin B), Ras-like

196   proteins (Rab38, KRas4A, KRas4B and HRas) and Prickle1 (**Figure 4A** and **Supplemental**

197   **Table S5**) (Ashar et al., 2000; Kho et al., 2004; Kim et al., 1990; Leung et al., 2007; Moudgil et

198   al., 2015; Onono et al., 2010; Palsuledesai et al., 2014; Storck et al., 2019; Strutt et al., 2013;

199   Varela et al., 2008). Apart from the Rab38-associated sequence (CAKS), every sequence was

200   completely modified by *Hs*FTase. CAKS is reported to be underprenylated in the context of

201   Rab38, which is consistent with our findings (Kohnke et al., 2013). Sequences ending in

202   methionine (CSIM, CAIM, CLIM, CIIM and CVIM) were fully modified in the presence of

203   *Hs*FTase yet partially modified in the absence of FTase (*ram1Δ*), suggesting that *Sc*GGTase-I

204   contributes to their prenylation. These observations are consistent with studies reporting that

205   *Sc*FTase, *Hs*FTase, and *Hs*GGTase-I recognize CaaM sequences, which we propose is a property

206   that extends to *Sc*GGTase-I as well (Caplin et al., 1994; Zhang et al., 1997).

207   The Ydj1 reporter system was also used to evaluate the prenylation of CaaX sequences

208   associated with human and swine viral proteins (**Figure 4B** and **Supplemental Table S5**). The

209   importance of prenylation in viral infection is an emerging line of inquiry for infectious disease

210   therapy but documentation of viral proteins prenylation is limited (Einav and Glenn, 2003;

211   Marakasova et al., 2017). All of the viral CaaX sequences evaluated were modified by *Hs*FTase.

212   These sequences were associated with influenza virus H1N1 PB2 (CRII); *Molluscum*

213   *contagiosum* virus subtype 1 MC155R (CVLM); human cytomegalovirus protein IRL9 (CRIQ);

214   Hepatitis Delta Virus L-HDAg (CRPQ); human adenovirus1 E1A (CLLS); hepatitis C virus non-

215   structural 5A protein (CSMS); human parainfluenza virus 3 hemagglutinin-neuraminidase

216   (CSQS); HIV NEF protein (CVVS); and African swine fever virus proteins Bcl-2 homolog

217   A179L (CNLI), X69R (CKCY) and I9R (CVFM). Of these, only hepatitis L-HDAg has been

218   biochemically characterized as being prenylated (Glenn et al., 1992). Several others are inferred

219   to be prenylated based on suppression of viral replication by statins (Pronin et al., 2021).

220   We also evaluated the prenylation status of CaaL/I/M sequences associated with prenylated

221   human proteins. Sequences adhering to consensus motif are considered targets of GGTase-I or

222   interchangeably by FTase or GGTase-I (Krzysiak et al., 2010; Trueblood et al., 1993; Zhang et

223   al., 1994). The CaaX sequences evaluated were from small GTPases (CDC42, RAC1, RAP1B,

224   RHOA and RHOB), G-protein gamma subunits (GBG5 and GBG12), myelin protein CN37, F-

225   box protein FBXL2 and anti-viral protein OAS1 p46 (De Angelis and Braun, 1994; Katayama et

226   al., 1991; Kawata et al., 1990; Kilpatrick and Hildebrandt, 2007; Onono et al., 2010; Soveg et al.,

227   2021; Storck et al., 2019; Wang et al., 2005; Wickenhagen et al., 2021). All Ydj1-CaaL/I/M

228   variants appeared to be fully prenylated in the presence of *Hs*FTase, with exception of CSFL that

229   does not adhere to the consensus sequence due to non-aliphatic amino acids at the a_1 and a_2

230   positions. Of note, a few sequences with non-aliphatic a_1 amino acids were fully prenylated (i.e.,

231   CTII, CKVL, and CQLL). Comparing band mobilities in the presence and absence of *Hs*FTase

232   indicated that several sequences were prenylated in a predominantly *Hs*FTase-dependent manner

233   (CKVL, CLLL, CLVL, CQLL, CSFL, and CVLL). For the remaining sequences, a smaller

234   portion of the population exhibited a mobility shift in the absence of *Hs*FTase (CTII, CIIL, CTIL

235   and CVIL), suggesting that these sequences are either naturally geranylgeranylated naturally

236   farnesylated but strongly subject to alternate prenylation when FTase is compromised (**Figure**

237   **4C**).

238   **_Hs_FTase modifies non-canonical length sequences**

239   The substrate recognition profile of FTase has recently been expanded to certain sequences one

240   amino acid longer or shorter than the tetrapeptide CaaX sequence (i.e., CaX and CaaaX). This

241   expanded specificity was first identified using a combination of yeast genetics and *in vitro*

242   biochemical analyses involving mammalian and yeast FTase (Ashok et al., 2020; Blanden et al.,

243   2018; Schey et al., 2021). Additional CaaaX sequences subject to farnesylation were

244   subsequently identified by *in vitro* screening of synthetic peptide libraries and by searches of the

245   human proteome ((Blanden et al., 2018; Schey et al., 2021) and this study). To extend these

246   observations to *Hs*FTase, previously studied Ydj1-CaX and -CaaaX variants were expressed in

247   the humanized FTase yeast strain and analyzed by gel-shift assay (**Figure 5**). One additional

248   CaX (CHA) sequence was also evaluated due to its association with SARS-CoV2 ORF7b.

249   The 16 CaX sequences evaluated exhibited varying degrees of farnesylation ranging from >90%

250   (CVI, CTI) to <25% (CLL and CHA), with half exhibiting >50% farnesylation (8 of 16) (**Figure**

251   **5A** and **Supplemental Table S1**). The farnesylation patterns were similar to that observed for

252   *Sc*FTase. The very weak modification of Ydj1-CHA, which was quantified to be ~8% of the

253   population, was not evident with SHA, consistent with the cysteine-dependent nature of this

254   modification, but it is unclear whether such a low level of modification it is likely to be

255   biologically significant for the biology of SARS-CoV2.

256   The 20 CaaaX sequences evaluated also exhibited varying degrees of farnesylation ranging from

257   >90% (e.g., CMIIM) to unfarnesylated (e.g., CASSQ), with nearly half exhibiting >50%

258   farnesylation (9 of 20) (**Figure 5B**). In most cases, *Sc*FTase and *Hs*FTase reactivities toward

259   Ydj1-CaaX sequences have been highly similar, with the extent of modification being

260 occasionally different for partially modified sequences (**Supplemental Table S1**). Here,

261 however, dramatic differences were observed for a few CaaaX sequences. Two sequences were

262 modified by *Hs*FTase but not *Sc*FTase: CQTGP (associated with GLCM1) and CSQGP

263 (SNED1). One sequence was fully modified by *Sc*FTase but <50% modified by *Hs*FTase:

264 CSLMQ (TCEA3) (**Figure 5C**). The species specificity differences observed with these CaaaX

265 sequences may indicate subtle differences in the FTase substrate binding pockets of these

266 enzymes that warrants future investigation.

267 This survey of CaX and CaaaX sequences reveals that *Hs*FTase can indeed modify non-

268 canonical length sequences in a cell-based system, albeit only a few exhibit full modification.

269 For the sequences associated with eukaryotic or viral proteins (see **Supplemental Table S5**), it

270 remains to be determined whether any are modified in their native context. Considering that

271 there are 988 CaX and 941 CaaaX human proteins in the UniProtKB/Swiss-Prot database (**Table**

272 **1**), it is possible that some of these will be prenylated.

The humanized FTase yeast strain can be used to identity novel *Hs*FTase target sequences

274 Two genetic screens, utilizing plasmid libraries based on distinct CaaX protein reporters (i.e.,

275 Ras and Ydj1), have comprehensively evaluated CaaX sequence space for reactivity with

276 *Sc*FTase (Kim et al., 2023; Stein et al., 2015). These genetic strategies are fully compatible with

277 the humanized FTase strain developed in this study and could be used to query CaaX sequence

278 space recognized by *Hs*FTase. As proof of principle of this possibility, we performed a

279 miniscreen by transforming the Ydj1-CaaX plasmid library into the humanized FTase strain and

280 recovered a random sampling of thermotolerant and temperature sensitive colonies from which

281 plasmids were recovered, sequenced, and evaluated by thermotolerance and gel-shift assays

282 (**Figure 6** and **Supplemental Table S1**). The results reveal a correlation between the ability to

283 support thermotolerance and being farnesylated by *Hs*FTase. The reciprocate is true for

284 temperature sensitivity and lack of farnesylation, except for the sequences CWIM and CWFC,

285 which were fully farnesylated yet temperature sensitive. The observations for CWIM and

286 CWFC are consistent with the profile of canonical CaaX sequences that temper the ability of

287 Ydj1 to support thermotolerance (i.e., fully-modified; farnesylated, cleaved, and

288 carboxylmethylated) (Berger et al., 2018; Hildebrandt et al., 2016b).

289   Studies of *Sc*FTase specificity have led to the development of predictive models for prenylation

290   (Berger et al., 2022; Kim et al., 2023). The more recent of these models was used to predict the

291   farnesylation status (positive and negative) of the randomly sampled CaaX sequences. The

292   predictions correlated well with empirical observations for positive and negative modification by

293   *Hs*FTase with the majority of sequences (20 of 26) being accurately predicted using rigorous

294   thresholds (>50% modification as determined by band quantitation was required for positive

295   classification; <10% modification was required for negative classification). For classification

296   purposes, CKRC was judged to be unmodified, consistent with its negative prediction, because

297   the gel-shift associated with this sequence also occurred in the absence of FTase (i.e., *ram1Δ*

298   background), indicating that it is not farnesylated (**Supplemental Figure S5**). Of the outlier

299   sequences, some were predicted to be modified, and indeed exhibited partial modification, but

300   the extent of their modification was below the threshold for positive classification (i.e., CWNA,

301   CWHS, CSNY and CPGH). By contrast, two outlier sequences that were predicted to be

302   modified were unmodified (i.e., CQLP and CFTP), perhaps indicating that a terminal proline is

303   unfavorable for farnesylation by *Hs*FTase, which has been previously reported (Kim et al., 2023;

304   Moores et al., 1991).

305   Among the randomly sampled sequences, only CPAA was found to exist in the human proteome

306   when querying the UniprotKB/SwissProt database. It is associated with two proteins: the ER-

307   localized DNase-1-like protein (P49184) and the extracellular laminin alpha subunit (Q16363).

308   While CPAA was reactive with *Hs*FTase, the subcellular locations of these human proteins likely

309   disqualify them from being substrates of cytosolic FTase. Nevertheless, our results suggest ~77%

310   accuracy when using a farnesylation prediction model developed using *Sc*FTase specificity data

311   to predict modification by *Hs*FTase (Kim et al., 2023). The substrate specificities of *Sc*FTase

312   and *Hs*FTase, although highly similar, are not identical, which prompts the need for future

313   studies aimed at fully evaluating CaaX sequence space in the context of *Hs*FTase. Such studies

314   are now possible with our humanized FTase yeast strain, and such investigations may better

315   refine the target profile of *Hs*FTase, potentially leading to the discovery of novel CaaX proteins.

316   **Interspecies complementation analysis of GGTase-I subunits**

12

317 To develop a yeast system for expressing *Hs*GGTase-I, studies were first performed to assess the

318 functional equivalence of *Sc*GGTase-I and *Hs*GGTase-I subunits. Because GGTase-I activity is

319 essential for yeast viability, strains lacking a *Sc*GGTase-I subunit can only be propagated when

320 complemented by plasmid-encoded copy of the missing gene (e.g., *ram2Δ* [*URA3 RAM2*]).

321 These strain backgrounds were further modified to introduce plasmid-encoded copies of one or

322 both orthologous *Hs*GGTase-I subunit genes FNTA and PGGT1B under different promoter

323 conditions. The strains were cultured, serially diluted, and spotted onto media containing 5-

324 fluroorotic acid (5FOA) that counter selects for the *URA3*-marked plasmids encoding *RAM2* or

325 *CDC43* in the parent strains. This strategy forced strains to contain either species matched or

326 mismatched subunits of GGTase-I in the absence or presence of FTase (*ram2Δ* and *cdc43Δ*

327 backgrounds, respectively).

328 The 5FOA analysis revealed, as observed for FTase, that neither FNTA nor PGGT1B alone

329 could complement for the absence of its yeast ortholog *ram2Δ* or *cdc43Δ*, respectively,

330 indicating that interspecies subunits do not form functional GGTase-I complexes (**Figure 7A**,

331 5FOA, 25 °C). This was observed whether FNTA and CDC43 (conditions **4** and **5**) or Ram2 and

332 PGGT1B (**8** and **9**) were co-expressed, and the result did not change when human subunits were

333 over-expressed using the *PGK1* strong constitutive promoter (**5** and **8**). Only when strains

334 producing both *Hs*GGTase-I subunits, whether expressed from the yeast orthologous promoters

335 (**3** and **7**) or the *PGK1* promoter (**2** and **6**), was growth equivalent to wildtype yeast (**1**). This

336 observation contrasts with the FTase situation where both *Hs*FTase subunits had to be expressed

337 from the *PGK1* promoter for functional complementation (**Supplemental Figure S1**). As

338 additional confirmation that yeast growth was specifically due to *Hs*GGTase-I activity, we

339 observed that *Hs*GGTase-I supported growth on 5FOA at 37 °C in the *cdc43Δ* but not *ram2Δ*

340 background (**Figure 7A**, 37 °C). FTase activity is required for growth at higher temperature (He

341 et al., 1991). The *cdc43Δ* strains (**6** and **7**) grew because they retain endogenous FTase activity

342 (i.e., Ram2/Ram1 complex), while the *ram2Δ* strains (**2** and **3**) failed to grow because they lack

343 FTase activity (i.e., Ram1 subunit only). Thus, it can be inferred that growth on 5FOA at 25 °C

344 in the *ram2Δ* background can be attributed entirely to *Hs*GGTase-I.

345 ***Hs*GGTase-I expressed in yeast modifies both canonical and non-canonical CaaX**

346 **sequences**

13

347   Evidence suggests that GGTase-I may have broader substrate specificity at the a_1 and a_2

348   positions akin to what has been observed for yeast and mammalian FTase (Kawata et al., 1990;

349   Kilpatrick and Hildebrandt, 2007; Lebowitz et al., 1997; Onono et al., 2010). We investigated

350   this issue more thoroughly using a three-plasmid system to examine geranylgeranylation of

351   plasmid-encoded Ydj1-CaaX variants in the context of *Hs*GGTase-I (**Figure 7B**). The strains

352   evaluated all lack endogenous FTase and Ydj1, but express either endogenous GGTase-I (*Sc*) or

353   plasmid-encoded *Hs*GGTase-I subunits from the orthologous *RAM2* and *CDC43* promoters (*Hs*)

354   or constitutive *PGK1* promoters (*PGKHs*). Gel-shift analysis revealed that neither *Sc*GGTase-I

355   nor *Hs*GGTase-I were able to modify Ydj1 harboring the CAHQ sequence that is associated with

356   the Ydj1 human ortholog DNAJA2 that is strictly a farnesylated sequence (Andres et al., 1997).

357   Other CaaX sequences (CNLI, CSFL, CVLL, CVIM, CIIM and CVLS) exhibited no or limited

358   modification by *Sc*GGTase-I, yet were better modified by *Hs*GGTase-I. This was more evident

359   when *Hs*GGTase-I subunit pairs were expressed using the strong *PGK1* promoter. These

360   observations suggest that *Hs*GGTase-I expressed in this yeast system is either more active or has

361   a different specificity than *Sc*GGTase-I, and that *Hs*GGTase-I indeed has the potential to modify

362   certain non-canonical CaaL/I/M sequences (e.g., CNLI and CSFL).

363   To further survey the geranylgeranylation potential of CaaX sequences, we evaluated a test set of

364   sequences that included 22 sequences that mostly matched the CaaL/I/M consensus. For this

365   analysis, we used the yeast system producing *Hs*GGTase-I from orthologous yeast promoters to

366   reduce the potential of over-expression artifacts (**Supplemental Figure S2C**). Most sequences

367   exhibited a gel-shift indicative of modification, but only a few exhibited complete modification

368   (i.e., CIIL, CTIL, CVIL, CVLL) or near-complete modification (CIIM, CVIM, CTII) (**Figure

369   7C**). Within this data set, we observed that the a_1 position influenced prenylation by *Hs*GGTase-

370   I. This is evident when comparing the CxIM set of sequences: CSIM, CAIM, and CLIM (~50%

371   modified) vs. CIIM and CVIM (100% modified). A similar observation was made when

372   comparing CxLL sequences: CLLL and CQLL (~50% modified) vs. CVLL (100% modified).

373   Sequences where the X position did not match the CaaL/I/M consensus (CAHQ, CVLS) were

374   unmodified by *Hs*GGTase-I.

375   **Human lamins and Pex19 CaaX sequences have distinct CaaX protease profiles**

376   The ability to humanize yeast for investigations of CaaX protein modifications can be extended

377   to studies of the human CaaX protease Rce1. This protease cleaves CaaX proteins that follow the

378   canonical modification pathway, which are subject to the coupled modifications of proteolysis

379   and carboxymethylation. Rce1 prefers to cleave prenylated CaaX sequences having an aliphatic

380   amino acid at a_2, and this substrate specificity is generally conserved among orthologs (Mokry et

381   al., 2009; Plummer et al., 2006). The Ste24 protease has also been referred to as a CaaX

382   protease, but its primary role is in protein quality control, and its substrates do not need to be

383   prenylated, unlike Rce1 (Ast et al., 2016; Boyartchuk et al., 1997; Hildebrandt et al., 2016a;

384   Runnebohm et al., 2020).

385   In yeast, the **a**-factor mating pheromone is a useful reporter of CaaX proteolysis that can be

386   coupled with expression of human Rce1 and ZMPSte24 for studies of target specificity in a cell-

387   based model (Mokry et al., 2009; Plummer et al., 2006). Such studies can be used to help

388   resolve the CaaX protease preferences of medically relevant human proteins. For example,

389   defects in the proteolytic processing of Prelamin A (CSIM) are associated with progeria-like

390   diseases (Barrowman et al., 2012b). Prelamin A is subject to two proteolytic events that yield

391   Lamin A: one within the CaaX sequence and another 15 amino acids from the C-terminus. Both

392   cleavage events have been attributed to ZMPSte24 (Barrowman et al., 2012a; Quigley et al.,

393   2013). With a humanized CaaX protease yeast model, however, we observe that **a**-factor-CSIM

394   is cleaved by *Hs*Rce1, not ZMPSte24, in accordance with more recent observations (**Figure 8**)

395   (Berger et al., 2022; Nie et al., 2020). We extended these studies to evaluate the cleavage of the

396   Lamin B CaaX sequence (CAIM), which was cleaved by both *Hs*Rce1 and ZMPSte24. This

397   result suggests that FTase inhibitors (FTIs) may impact the CaaX processing of both lamins,

398   while Rce1 inhibitors are likely to differentially impact Prelamin A and Lamin B processing. We

399   also examined cleavage of the human peroxisomal chaperone Pex19 CaaX sequence.

400   Farnesylation of Pex19 is critical for its interaction with client proteins, and mutations of Pex19

401   unrelated to its CaaX sequence are associated with Zellweger syndrome (Emmanouilidis et al.,

402   2017; Matsuzono et al., 1999). Human Pex19 (CLIM) and yeast Pex19 (CKQQ) have strikingly

403   different CaaX sequences despite moderate homology (i.e., 21% identity; 48% similarity)

404   (Madeira et al., 2022). Both sequences are fully prenylated in the context of either *Hs*FTase or

405   *Sc*FTase (**Figure 4A** and **Supplemental Figure S4**). Using **a**-factor-CaaX variants harboring

406   these sequences, CLIM was observed to be cleaved by both *Hs*RCE1 and ZMPSte24, whereas

407   the non-canonical CKQQ sequence was not. This result suggests that Pex19 proteins have

408   evolved to have C-termini with distinct biophysical properties: canonical for human Pex19 and

409   only isoprenylated for yeast Pex19. The underlying reasons for these differences remain

410   unknown. Nonetheless, our studies with lamins and Pex19 fully support the utility of the

411   humanized CaaX protease model system for expanding studies of CaaX protein post-

412   translational modifications (PTMs) beyond the initial prenylation step. Such studies could prove

413   useful for predicting the potential effects of inhibiting the Rce1 CaaX protease, which would

414   impact a narrower range of CaaX protein targets than prenyltransferase inhibitors.

Discussion

416   We report the development of yeast strains that can be used for systematic characterization of

417   prenylation by human FTase and GGTase-I. The humanized FTase strain, with subunits FNTA

418   and FNTB integrated into the yeast genome, was phenotypically equivalent to yeast expressing

419   native FTase in four functional tests: 1) production of **a**-factor mating pheromone, 2) Ras2

420   localization 3) Ydj1-based thermotolerance, and 4) Ydj1 farnesylation. Thus, the humanized

421   FTase yeast strain provides *in vivo* FTase activity levels compatible for relatively rapid

422   characterization of candidate CaaX sequences and heterologously expressed human CaaX

423   proteins that may be targets for farnesylation. Moreover, the humanized FTase yeast strain

424   provides a cell-based system that overcomes concerns associated with *in vitro* farnesylation

425   assays that depend on chemically modified substrates and unnatural enzyme and substrate

426   amounts. For example, the annexin A2 CGGDD extended CaaaX sequence has been reported as

427   farnesylated with methods involving metabolic labeling with an azido-farnesyl analog (Kho et

428   al., 2004), but this sequence is unmodified by human FTase in our cell-based system (**Figure**

429   **5C**). The convenience of the yeast system for heterologous protein expression makes it ideal for

430   coupling with other methods, such as mass-spectrometry, for confidently validating the

431   prenylation status of candidate CaaX proteins.

432   Limited comparative data exists for the specificities of mammalian FTase relative to *Sc*FTase. *In*

433   *vitro,* rat FTase and *Sc*FTase and exhibit similar specificities when evaluated against a CVa$_2$X

434   peptide library (Wang et al., 2014). Our *in vivo* results confirm and further extend such

435   observations to reveal that *Hs*FTase expressed in yeast and native *Sc*FTase have a striking degree

16

436 of substrate conservation (see **Supplemental Figure S4**, **Supplemental Table S1**). This is most

437 evident in the ability of both enzymes to similarly prenylate canonical and prenylation-only

438 CaaX sequences. Thus, *Hs*FTase also appears to possess the broadened ability to modify non-

439 canonical sequences (i.e., sequences without aliphatic amino acids at the a_1 and a_2 positions),

440 which was initially reported for *Sc*FTase (Berger et al., 2018). These findings indicate that

441 farnesylation prediction algorithms developed using *Sc*FTase should work reasonably well for

442 predicting *Hs*FTase specificity (Kim et al., 2023). The conservation between human and yeast

443 FTases extends to prenylation of non-standard length sequences that are one amino acid shorter

444 or longer than the conventional tetrapeptide CaaX sequence, although species specific

445 differences in substrate recognition of longer CaaaX sequences was observed.

446 The humanized GGTase-I strain, with subunits FNTA and PGGT1B expressed from low copy

447 plasmids and driven by the orthologous yeast promoters, was phenotypically equivalent to yeast

448 expressing native GGTase-I in supporting viability. The humanized GGTase-I strain, however,

449 displayed more robust activity than endogenous yeast GGTase-I in modifying Ydj1-CaaL/I/M

450 variants. This observation could be due to higher GGTase-I enzyme levels and/or subtle

451 specificity differences between yeast and human enzymes. Human GGTase-I prenylated a wide

452 range of CaaL/I/M sequences and did not prenylate CaaS/Q sequences, in alignment with

453 expectations. One feature that was conserved across species was the ability of GGTase-I to

454 alternatively prenylate normally farnesylated sequences. This typically occurs when FTase

455 activity is reduced through action of FTIs, and in our case, when the FTase activity was

456 genetically ablated. The observation that yeast and human FTase and GGTase-I can alternatively

457 prenylate Ras sequences CIIM and CVIM when using Ydj1 or GFP-Ras2 reporters

458 (**Supplemental Figure S6**) demonstrates that recognition of these sequences by both

459 prenyltransferases is transferable and evolutionarily conserved between yeast and human

460 enzymes, and likely across other species as well.

461 The scope of potentially prenylated proteins in protein databases is expansive with over 6000

462 annotated proteins in eukaryotes and viruses ending in Cxxx. When expanded to 3-mer and 5-

463 mer length sequences, this number is over 15,000 (see **Table 1**). Not accounted for in this table,

464 is the potential number of prokaryotic CaaX proteins. While prokaryotes lack protein prenylation

465 machinery, there is evidence that some pathogenic bacteria, such as *Legionella pneumophila* and

17

466   *Salmonella typhimurium,* encode CaaX proteins that are prenylated by host enzymes as part of

467   their infectious life cycle (Ivanov et al., 2010; Reinicke et al., 2005). Thus, a reliable prediction

468   algorithm and reporter systems to identify and verify the subpopulation of CaaX sequences that

469   are likely to be modified by either FTase or GGTase-I will be a key step toward defining the

470   prenylome across many different organisms.

471   Viral genomes encode many CaaX proteins that might be prenylated by human FTase and/or

472   GGTase-I. We have evaluated several such sequences using our system, with results confirming

473   instances of previously reported prenylation or indicating compatibility for prenylation. For

474   example, we observed that the CaaX sequence of Hepatitis Delta Virus Large Delta antigen (L-

475   HDAg; CRPQ) is modified by human and yeast FTases, but not by GGTase-I. Moreover, we

476   observed that the CRPQ sequence is neither cleaved nor carboxylmethylated, consistent with its

477   non-canonical sequence (see **Figure 4** and **Supplemental Figures 2 and 3**). Prenylation of L-

478   HDAg is required for virion assembly, and the FTI Lonafarnib is currently in Phase 3 clinical

479   trials for use in combination treatments for Hepatitis D infections (Khalfi et al., 2023; Koh et al.,

480   2015; Yardeni et al., 2022). We also determined that the CaaX sequence of human

481   cytomegalovirus protein of unknown function IRL9 (CRIQ) can be farnesylated, cleaved and

482   carboxymethylated. The modifications of IRL9 have not been previously reported, so it is a good

483   candidate for additional investigations related to its prenylation status and impact of PTMs to

484   virion formation. Other viral CaaX sequences CRII (Influenza virus H1N1 protein PB2), CVLM

485   (Molluscum contagiosum virus protein MC155R) and CNLI (ASFV protein A179L) were

486   substrates of both *Hs*FTase and *Hs*GGTase-I in our system. If these sequences are prenylated in

487   their native context, dual prenyltransferase inhibitors might have better utility for blocking

488   modification. Given that all the viral CaaX sequences evaluated in our study were targets for

489   prenylation, it is prudent to consider the role that the prenylation of viral proteins may have on

490   viral propagation and infection. The ability to readily assess the prenylation status of viral CaaX

491   sequences afforded by our cell-based system could provide the necessary evidence for new

492   investigations of viral biology or viral therapies in human and veterinary medicine involving

493   FTIs, geranylgeranyltransferase inhibitors (GGTIs), dual prenyltransferase inhibitors (DPIs), and

494   possibly CaaX protease and ICMT inhibitors as well.

495   Our system is well-suited for assessing the prenylation status of human proteins as supported by

496   the modification of heterologously expressed human HRas61 and DNAJA2. An important caveat

497   to consider is that SDS-PAGE gel-shifts do not universally occur for all prenylated proteins,

498   which is why Ydj1 is such a great reporter protein for testing CaaX sequences. Unfortunately,

499   our system does not exclude the possibility of a CaaX sequence being reactive in the context of

500   Ydj1, but unreactive its native context, for a myriad of reasons (e.g., structurally inaccessible C-

501   terminus, localization of protein inaccessible to cytosolic prenyltransferases, alternate cysteine

502   modifications such as disulfide bonding, etc.). Therefore, positive results with our system should

503   be coupled with additional validation of prenylation in native contexts. Nonetheless, the ease and

504   convenience of the humanized FTase and GGTase-I yeast strains that we have developed are an

505   important and valuable new resource for initial investigations into evaluating the prenylation

506   potential of a wide array of CaaX sequences.

507

508   **Materials and Methods**

509   Yeast strains: The humanized prenyltransferase strains are summarized in **Supplemental Figure**

510   **S2**. All yeast strains used in this study are listed in **Supplemental Table S2**. Detailed

511   descriptions of strain constructions can be found in the **Supplemental Methods** file. Yeast were

512   typically cultured in standard liquid and solid yeast media unless otherwise noted. For expression

513   of Myc-HRas61 from the inducible *MET25* promoter (p-05547) in methionine auxotroph strains

514   (i.e., yWS2544 and yWS3186), yeast were first cultured in SC-leucine containing 20 µg/ml

515   methionine to late log phase, washed, and resuspended in SC-leucine containing 2 µg/ml

516   methionine to allow for both growth and induction of the *MET25* promoter.

517   New strains were typically created for this study by standard genetic manipulations starting with

518   commercially available haploid and heterozygous diploid genomic deletions. KAN^R and NAT^R

519   marked gene replacements were confirmed by growth on YPD containing G418 (200 µg/ml;

520   Research Products International) or nourseothricin (100 µg/ml; GoldBio), respectively. All gene

521   replacements were further checked by PCR to confirm the presence of the knockout at the

522   correct locus and absence of the wild-type open reading frame. Plasmids were introduced into

523   strains via a lithium acetate-based transformation procedure (Elble, 1992). Yeast sporulation was

19

524   carried out in a solution of 2% potassium acetate, 0.25% yeast extract, and 0.1% dextrose. Spore

525   enrichment and random spore analysis followed published methods (Rockmill et al., 1991). For

526   the humanized FTase strains (yWS3186 and yWS3220), P_{PGK1}-$FNTB$ was integrated at the

527    $RAM1$ locus, replacing the open reading frame, using a loop-in loop out strategy, and P_{PGK1}-

528    $FNTA$ was integrated at the $his3\Delta1$ locus by homologous recombination using a $HIS3$-based

529   integrative plasmid (Schey et al., 2023).

530   Plasmids: The plasmids used in this study are listed in **Supplemental Table S3**. Detailed

531   descriptions of plasmid construction can be found in the Supplemental Methods file. Plasmids

532   were analyzed by diagnostic restriction digest and DNA sequencing (Eurofins Genomics,

533   Louisville, KY) to verify the entire open reading frame and surrounding sequence. Plasmids

534   recovered from the Ydj1-CaaX Trimer20 library are described elsewhere (Kim et al., 2023). New

535   plasmids encoding Ydj1-CaaX and **a**-factor-CaaX (encoded by $MFA1$ gene) variants were made

536   by PCR-directed plasmid based recombinational cloning as previously described (Berger et al.,

537   2018; Oldenburg et al., 1997). Plasmids with GFP-Ras2-CaaX variants were generated by

538   QuikChange site-directed mutagenesis. Plasmids encoding HsFTase and HsGGTase-I subunits

539   were created in multiple steps. First, the open reading frames (ORFs) and flanking 5´ and 3´

540   sequences of yeast prenyltransferase subunits were PCR-amplified from strain BY4741 and

541   subcloned into the multicloning sites of appropriate pRS series vectors (Sikorski and Hieter,

542   1989). In parallel, synthetic cDNAs for human FNTA, FNTB and PGGT1B that were codon

543   optimized for $S. cerevisiae$ were subcloned into the PstI and XhoI sites of pBluescriptII KS(-); all

544   cDNAs were commercially obtained (GenScript). The human ORFs were engineered to also

545   have 39 bp of flanking sequence on both the 5´ and 3´ends that equivalently matched the

546   flanking sequences of the orthologous yeast ORFs. Next, DNA fragments encoding the human

547   ORFs and yeast flanking sequences were used with recombination-based methods for direct gene

548   replacement of the plasmid-encoded yeast ORFs. The $PGK1$ promoter was amplified and used

549   to replace the orthologous yeast promoters by similar recombination-based methods as described

550   in **Supplemental Materials**. To change selectable markers, the various FTase and GGTase-I

551   promoter-containing segments were subcloned as XhoI-SacI fragments into different pRS vector

552   backbones by conventional ligation-based cloning.

553   Temperature sensitivity assay: Thermotolerance assays were performed as previously described

554   (Blanden et al., 2018; Hildebrandt et al., 2016b). In brief, plasmid-transformed strains were

555   cultured in appropriate selective synthetic drop-out (SC-) liquid media to saturation (25 °C, 24

556   hours); strains without plasmids were cultured in SC complete media. Cultures were serially

557   diluted into H_2O (10-fold dilutions), and dilutions replica pinned onto YPD plates. Plates were

558   incubated (25 °C for 72 hours; 37 °C for 48 hours; 40 °C and 41 °C for 72 hours) then digitally

559   imaged using a Canon flat-bed scanner (300 dpi; grayscale; TIFF format).

560   <u>Yeast lysate preparations and immunoblots:</u> Cell-mass equivalents of log-phase yeast (A_{600}

561   0.95-1.1) cultured in appropriate selective SC- liquid media were harvested by centrifugation,

562   washed with water, and processed by alkaline hydrolysis and TCA precipitation (Kim et al.,

563   2005). Total protein precipitates were resuspended in urea-containing Sample Buffer (250 mM

564   Tris, 6 M urea, 5% β-mercaptoethanol, 4% SDS, 0.01% bromophenol blue, pH 8), and analyzed

565   by SDS-PAGE (9.5%) followed by immunoblotting. Blots were processed according to standard

566   protocols. Antibodies used for Western blots were rabbit anti-Ydj1 polyclonal (1:10,000

567   dilution; gift from A. Caplan); mouse anti-c-Myc 9E10 monoclonal (1:1000 dilution, Santa Cruz

568   Biotech. #sc-40); mouse anti-GFP B-2 monoclonal (1:500, Santa Cruz Biotech. # sc-9996);

569   mouse anti-DnaJA2(7) monoclonal (1:500 dilution, Santa Cruz Biotech. sc-136515); mouse anti-

570   HIS his.h8 monoclonal (1:1000 dilution, VWR #101981-852); goat HRP-anti-rabbit and goat

571   HRP-anti-mouse (1:1000 dilutions, Kindle Biosciences, LLC #R1006 and R1005, respectively).

572   Immunoblots were developed with ECL reagent (ProSignal Pico ECL Spray or Kindle

573   Biosciences KwikQuant Western Blot Detection Kit) and images were digitally captured using

574   the KwikQuant Imager system (Kindle Biosciences). Adobe Photoshop was used for cropping

575   and rotating of images; no other image adjustments were applied.

576   Prenylation of Ydj1-CaaX was quantified using ImageJ and multiple exposures having good

577   dynamic range of band intensities. Percent prenylation was calculated as the intensity of the

578   lower (prenylated band) divided by total intensity of the prenylated and unprenylated (upper)

579   bands. Data presented in **Supplemental Table S1** represent the averages of biological

580   replicates. For duplicate samples, values are reported as an average and associated range. For

581   multiplicate samples, the values are reported as an average and standard error of the mean

582   (SEM).

583 Yeast mating assay: Qualitative and quantitative yeast mating assays were performed as detailed

584 previously (Berger et al., 2018). In brief, *MAT***a** test strains and the *MAT*α strain (IH1793) were

585 cultured to saturation at 25 °C in appropriate selective SC- media and YPD liquid media,

586 respectively. Cultures were normalized by dilution with fresh media (A$_{600}$ 1.0), mixed 1:9

587 (*MAT***a**:*MAT*α) in individual wells of a 96-well plate, and cell mixtures subject to 10-fold serial

588 dilution using the *MAT*α cell suspension as the diluent. For qualitative analyses, each dilution

589 series was replica pinned onto SC-lysine and minimal SD solid media. For quantitative analysis,

590 a portion of a dilution mixture was spread onto SC-lysine and SD plates in duplicate, and

591 colonies counted after plate incubation (72 hours, 30 °C). The SC-lysine cell count reports on the

592 total number of *MAT***a** haploid cells initially in the mixture while the SD cell count reports on the

593 number of mating events (i.e., diploids). Mating efficiencies were normalized to an **a**-factor

594 (*MFA1)* positive control within each experiment.

595 Microscopy: Imaging was performed as detailed previously (Ravishankar et al., 2023). In brief,

596 yeast transformed with *CEN URA3 P$_{Ydj1}$-GFP-RAS2-CaaX* variants were cultured to late log

597 (A$_{600}$ 0.8-1) in SC-uracil liquid media and viewed using a Zeiss Axio Observer microscope

598 equipped with fluorescence optics (Plan Apochromat 63X/1.4 N.A objective). Images were

599 captured using AxioVision software and minor image adjustments performed using Adobe

600 Photoshop.

601 Humanized yeast miniscreen for identification of Ydj1-CaaX variants: yWS3186 was

602 transformed with the Ydj1-CaaX plasmid library (pWS1775), plated onto SC-uracil solid media,

603 and incubated 4 days at 25 °C. Single colonies of varying size were individually cultured and

604 subject to the temperature sensitivity assay described above except that 3 spots of 20-fold serial

605 dilutions were prepared. Growth at 41 °C was scored on a scale of 0 to 5 relative to control

606 strains yWS3311 (Ydj1-CASQ, score of 5) and yWS3312 (Ydj1-SASQ, score of 0). Plasmids

607 were recovered from candidates scoring 0 (n=11) and candidates scoring 5 (n=15), sequenced to

608 identify the CaaX sequence, and retransformed into yWS3186 for retesting by the temperature

609 sensitivity assay (10-fold dilutions) and SDS-PAGE gel-shift assay.

610 5-fluroorotic acid (5FOA) assay: BY4741, yWS3106 and yWS3109 were transformed with

611 combinations of *HIS3* and *LEU2* based plasmids carrying *Hs*FNTA, *Hs*PGGT1B, and/or empty

22

612   vector plasmids such that all strains had the same selectable markers. Strains cultured on SC-

613   histidine-leucine-uracil solid media were used to inoculate SC-histidine-leucine liquid media.

614   After incubation (25 °C, 24 hours), cultures were normalized with fresh media (A_{600} 2.0), added

615   to wells of a 96 well plate, serial diluted 8-fold with H_2O as the diluent, and the dilution series

616   pinned onto SC complete solid media containing 1 mg/ml 5-fluroorotic acid (5FOA).

617   Search for CaaX sequences: Scan Prosite (https://prosite.expasy.org/scanprosite/) was used to

618   search for CaaX sequences in *Homo sapiens* and viruses in the UniProtKB/Swiss-Prot database

619   using the search strings "CXXX>", "C{C}XXX>", or "{C}CXX>" (search performed

620   07/12/2023). For certain CaaaX and CaX and sequences that were studied in previous

621   publications but have no human or virus associated protein in the annotated UniProtKB/Swiss-

622   Prot database, the search was expanded UniProtKB/TrEMBL database, inclusive of all

623   eukaryotes.

624

629   **Competing interests:** none

632   **Data Availability:** Strains and plasmids generated for this study are available upon request.

633

References

Adari, H., Lowy, D. R., Willumsen, B. M., Der, C. J. and McCormick, F. (1988). Guanosine triphosphatase activating protein (GAP) interacts with the p21 ras effector binding domain. *Science* **240**, 518-21.

Anderegg, R., Betz, R., Carr, S., Crabb, J. and Duntze, W. (1988). Structure of *Saccharomyces cerevisiae* mating hormone **a**-factor: identification of S-farnesyl cysteine as a structural component. *J Biol Chem* **263**, 18236-18240.

Andres, D. A., Shao, H., Crick, D. C. and Finlin, B. S. (1997). Expression cloning of a novel farnesylated protein, RDJ2, encoding a DnaJ protein homologue. *Arch Biochem Biophys* **346**, 113-24.

Ashar, H. R., James, L., Gray, K., Carr, D., Black, S., Armstrong, L., Bishop, W. R. and Kirschmeier, P. (2000). Farnesyl transferase inhibitors block the farnesylation of CENP-E and CENP-F and alter the association of CENP-E with the microtubules. *J Biol Chem* **275**, 30451-7.

Ashok, S., Hildebrandt, E. R., Ruiz, C. S., Hardgrove, D. S., Coreno, D. W., Schmidt, W. K. and Hougland, J. L. (2020). Protein Farnesyltransferase Catalyzes Unanticipated Farnesylation and Geranylgeranylation of Shortened Target Sequences. *Biochemistry* **59**, 1149-1162.

Ast, T., Michaelis, S. and Schuldiner, M. (2016). The protease Ste24 clears clogged translocons. *Cell* **164**, 103-14.

Barrowman, J., Hamblet, C., Kane, M. S. and Michaelis, S. (2012a). Requirements for efficient proteolytic cleavage of prelamin A by ZMPSTE24. *PLoS One* **7**, e32120.

Barrowman, J., Wiley, P. A., Hudon-Miller, S. E., Hrycyna, C. A. and Michaelis, S. (2012b). Human ZMPSTE24 disease mutations: residual proteolytic activity correlates with disease severity. *Hum Mol Genet* **21**, 4084-93.

Berger, B. M., Kim, J. H., Hildebrandt, E. R., Davis, I. C., Morgan, M. C., Hougland, J. L. and Schmidt, W. K. (2018). Protein isoprenylation in yeast targets COOH-terminal sequences not adhering to the CaaX consensus. *Genetics* **210**, 1301-1316.

Berger, B. M., Yeung, W., Goyal, A., Zhou, Z., Hildebrandt, E. R., Kannan, N. and Schmidt, W. K. (2022). Functional classification and validation of yeast prenylation motifs using machine learning and genetic reporters. *PLoS One* **17**, e0270128.

Blanden, M. J., Suazo, K. F., Hildebrandt, E. R., Hardgrove, D. S., Patel, M., Saunders, W. P., Distefano, M. D., Schmidt, W. K. and Hougland, J. L. (2018). Efficient farnesylation of an extended C-terminal C(x)$_3$X sequence motif expands the scope of the prenylated proteome. *J Biol Chem* **293**, 2770-2785.

Boyartchuk, V. L., Ashby, M. N. and Rine, J. (1997). Modulation of Ras and **a**-factor function by carboxyl-terminal proteolysis. *Science* **275**, 1796-800.

Brachmann, C. B., Davies, A., Cost, G. J., Caputo, E., Li, J., Hieter, P. and Boeke, J. D. (1998). Designer deletion strains derived from Saccharomyces cerevisiae S288C: a useful set of strains and plasmids for PCR-mediated gene disruption and other applications. *Yeast* **14**, 115-32.

Cadinanos, J., Varela, I., Mandel, D., Schmidt, W. K., Díaz-Perales, A., López-Otín, C. and JMP, F. (2003). AtFACE-2, a prenylated-protein protease from *Arabidopsis thaliana* related to Ras converting enzymes. *J Biol Chem* **278**, 42091-7.

Campbell, S. L. and Philips, M. R. (2021). Post-translational modification of RAS proteins. *Curr Opin Struct Biol* **71**, 180-192.

Caplin, B. E., Hettich, L. A. and Marshall, M. S. (1994). Substrate characterization of the Saccharomyces cerevisiae protein farnesyltransferase and type-I protein geranylgeranyltransferase. *Biochim Biophys Acta* **1205**, 39-48.

Cox, A. D., Der, C. J. and Philips, M. R. (2015). Targeting RAS Membrane Association: Back to the Future for Anti-RAS Drug Discovery? *Clin Cancer Res* **21**, 1819-27.

De Angelis, D. A. and Braun, P. E. (1994). Isoprenylation of brain 2',3'-cyclic nucleotide 3'-phosphodiesterase modulates cell morphology. *J Neurosci Res* **39**, 386-97.

Dong, X., Mitchell, D. A., Lobo, S., Zhao, L., Bartels, D. J. and Deschenes, R. J. (2003). Palmitoylation and plasma membrane localization of Ras2p by a nonclassical trafficking pathway in Saccharomyces cerevisiae. *Mol Cell Biol* **23**, 6574-84.

Einav, S. and Glenn, J. S. (2003). Prenylation inhibitors: a novel class of antiviral agents. *J Antimicrob Chemother* **52**, 883-6.

Elble, R. (1992). A simple and efficient procedure for transformation of yeasts. *Biotechniques* **13**, 18-20.

Emmanouilidis, L., Schutz, U., Tripsianes, K., Madl, T., Radke, J., Rucktaschel, R., Wilmanns, M., Schliebs, W., Erdmann, R. and Sattler, M. (2017). Allosteric modulation of peroxisomal membrane protein recognition by farnesylation of the peroxisomal import receptor PEX19. *Nat Commun* **8**, 14635.

Farnsworth, C. L., Marshall, M. S., Gibbs, J. B., Stacey, D. W. and Feig, L. A. (1991). Preferential inhibition of the oncogenic form of RasH by mutations in the GAP binding/"effector" domain. *Cell* **64**, 625-33.

Glenn, J. S., Watson, J. A., Havel, C. M. and White, J. M. (1992). Identification of a prenylation site in delta virus large antigen. *Science* **256**, 1331-3.

Hancock, J. F., Magee, A. I., Childs, J. E. and Marshall, C. J. (1989). All ras proteins are polyisoprenylated but only some are palmitoylated. *Cell* **57**, 1167-77.

Hartman, H. L., Hicks, K. A. and Fierke, C. A. (2005). Peptide specificity of protein prenyltransferases is determined mainly by reactivity rather than binding affinity. *Biochemistry* **44**, 15314-24.

He, B., Chen, P., Chen, S. Y., Vancura, K. L., Michaelis, S. and Powers, S. (1991). *RAM2*, an essential gene of yeast, and *RAM1* encode the two polypeptide components of the farnesyltransferase that prenylates **a**-factor and Ras proteins. *Proc Natl Acad Sci USA* **88**, 11373-7.

Hildebrandt, E. R., Arachea, B. T., Wiener, M. C. and Schmidt, W. K. (2016a). Ste24p Mediates Proteolysis of Both Isoprenylated and Non-prenylated Oligopeptides. *J Biol Chem* **291**, 14185-98.

Hildebrandt, E. R., Cheng, M., Zhao, P., Kim, J. H., Wells, L. and Schmidt, W. K. (2016b). A shunt pathway limits the CaaX processing of Hsp40 Ydj1p and regulates Ydj1p-dependent phenotypes. *eLife* **5**, e15899.

Hougland, J. L., Hicks, K. A., Hartman, H. L., Kelly, R. A., Watt, T. J. and Fierke, C. A. (2010). Identification of novel peptide substrates for protein farnesyltransferase reveals two substrate classes with distinct sequence selectivities. *J Mol Biol* **395**, 176-90.

Ivanov, S. S., Charron, G., Hang, H. C. and Roy, C. R. (2010). Lipidation by the host prenyltransferase machinery facilitates membrane localization of Legionella pneumophila effector proteins. *J Biol Chem* **285**, 34686-98.

Jeong, A., Auger, S. A., Maity, S., Fredriksen, K., Zhong, R., Li, L. and Distefano, M. D. (2022). In Vivo Prenylomic Profiling in the Brain of a Transgenic Mouse Model of Alzheimer's Disease Reveals Increased Prenylation of a Key Set of Proteins. *ACS Chem Biol* **17**, 2863-2876.

Katayama, M., Kawata, M., Yoshida, Y., Horiuchi, H., Yamamoto, T., Matsuura, Y. and Takai, Y. (1991). The posttranslationally modified C-terminal structure of bovine aortic smooth muscle rhoA p21. *J Biol Chem* **266**, 12639-45.

Kawata, M., Farnsworth, C. C., Yoshida, Y., Gelb, M. H., Glomset, J. A. and Takai, Y. (1990). Posttranslationally processed structure of the human platelet protein smg p21B: evidence for geranylgeranylation and carboxyl methylation of the C-terminal cysteine. *Proc Natl Acad Sci USA* **87**, 8960-4.

Khalfi, P., Kennedy, P. T., Majzoub, K. and Asselah, T. (2023). Hepatitis D virus: Improving virological knowledge to develop new treatments. *Antiviral Res* **209**, 105461.

Kho, Y., Kim, S. C., Jiang, C., Barma, D., Kwon, S. W., Cheng, J., Jaunbergs, J., Weinbaum, C., Tamanoi, F., Falck, J. et al. (2004). A tagging-via-substrate technology for detection and proteomics of farnesylated proteins. *Proc Natl Acad Sci USA* **101**, 12479-84.

Kilpatrick, E. L. and Hildebrandt, J. D. (2007). Sequence dependence and differential expression of Ggamma5 subunit isoforms of the heterotrimeric G proteins variably processed after prenylation in mammalian cells. *J Biol Chem* **282**, 14038-47.

Kim, J. H., Hildebrandt, E. R., Sarkar, A., Yeung, W., Waldon, R. A., Kannan, N. and Schmidt, W. K. (2023). A comprehensive in vivo screen of yeast farnesyltransferase activity reveals broad reactivity across a majority of CXXX sequences. *G3 (Bethesda)* **7**, jkad094.

Kim, R., Rine, J. and Kim, S. H. (1990). Prenylation of mammalian Ras protein in Xenopus oocytes. *Mol Cell Biol* **10**, 5945-9.

Kim, S., Lapham, A., Freedman, C., Reed, T. and Schmidt, W. (2005). Yeast as a tractable genetic system for functional studies of the insulin-degrading enzyme. *J Biol Chem* **280**, 27481-27490.

Koh, C., Canini, L., Dahari, H., Zhao, X., Uprichard, S. L., Haynes-Williams, V., Winters, M. A., Subramanya, G., Cooper, S. L., Pinto, P. et al. (2015). Oral prenylation inhibition with lonafarnib in chronic hepatitis D infection: a proof-of-concept randomised, double-blind, placebo-controlled phase 2A trial. *Lancet Infect Dis* **15**, 1167-1174.

Kohnke, M., Delon, C., Hastie, M. L., Nguyen, U. T., Wu, Y. W., Waldmann, H., Goody, R. S., Gorman, J. J. and Alexandrov, K. (2013). Rab GTPase prenylation hierarchy and its potential role in choroideremia disease. *PLoS One* **8**, e81758.

Krishnankutty, R. K., Kukday, S. S., Castleberry, A. J., Breevoort, S. R. and Schmidt, W. K. (2009). Proteolytic processing of certain CaaX motifs can occur in the absence of the Rce1p and Ste24p CaaX proteases. *Yeast* **26**, 451-463.

Krzysiak, A. J., Aditya, A. V., Hougland, J. L., Fierke, C. A. and Gibbs, R. A. (2010). Synthesis and screening of a CaaL peptide library versus FTase reveals a surprising number of substrates. *Bioorg Med Chem Lett* **20**, 767-70.

Lane, K. T. and Beese, L. S. (2006). Thematic review series: lipid posttranslational modifications. Structural biology of protein farnesyltransferase and geranylgeranyltransferase type I. *J Lipid Res* **47**, 681-99.

Lebowitz, P. F., Casey, P. J., Prendergast, G. C. and Thissen, J. A. (1997). Farnesyltransferase inhibitors alter the prenylation and growth-stimulating function of RhoB. *J Biol Chem* **272**, 15591-4.

Leung, K. F., Baron, R., Ali, B. R., Magee, A. I. and Seabra, M. C. (2007). Rab GTPases containing a CAAX motif are processed post-geranylgeranylation by proteolysis and methylation. *J Biol Chem* **282**, 1487-1497.

Madeira, F., Pearce, M., Tivey, A. R. N., Basutkar, P., Lee, J., Edbali, O., Madhusoodanan, N., Kolesnikov, A. and Lopez, R. (2022). Search and sequence analysis tools services from EMBL-EBI in 2022. *Nucleic Acids Res* **50**, W276-W279.

Marakasova, E. S., Eisenhaber, B., Maurer-Stroh, S., Eisenhaber, F. and Baranova, A. (2017). Prenylation of viral proteins by enzymes of the host: Virus-driven rationale for therapy with statins and FT/GGT1 inhibitors. *Bioessays* **39**, 1700014.

Matsuzono, Y., Kinoshita, N., Tamura, S., Shimozawa, N., Hamasaki, M., Ghaedi, K., Wanders, R. J., Suzuki, Y., Kondo, N. and Fujiki, Y. (1999). Human PEX19: cDNA cloning by functional complementation, mutation analysis in a patient with Zellweger syndrome, and potential role in peroxisomal membrane assembly. *Proc Natl Acad Sci USA* **96**, 2116-21.

Maurer-Stroh, S., Washietl, S. and Eisenhaber, F. (2003). Protein prenyltransferases. *Genome Biol* **4**, 212.

Michaelson, D., Ali, W., Chiu, V. K., Bergo, M., Silletti, J., Wright, L., Young, S. G. and Philips, M. (2005). Postprenylation CAAX processing is required for proper localization of Ras but not Rho GTPases. *Mol Biol Cell* **16**, 1606-16.

Mohammed, I., Hampton, S. E., Ashall, L., Hildebrandt, E. R., Kutlik, R. A., Manandhar, S. P., Floyd, B. J., Smith, H. E., Dozier, J. K., Distefano, M. D. et al. (2016). 8-Hydroxyquinoline-based inhibitors of the Rce1 protease disrupt Ras membrane localization in human cells. *Bioorg Med Chem* **24**, 160-78.

Mokry, D. Z., Manandhar, S. P., Chicola, K. A., Santangelo, G. M. and Schmidt, W. K. (2009). Heterologous expression studies of *Saccharomyces cerevisiae* reveal two distinct trypanosomatid CaaX protease activities and identify their potential targets. *Eukaryot Cell* **8**, 1891-900.

Moores, S. L., Schaber, M. D., Mosser, S. D., Rands, E., O'Hara, M. B., Garsky, V. M., Marshall, M. S., Pompliano, D. L. and Gibbs, J. B. (1991). Sequence dependence of protein isoprenylation. *J Biol Chem* **266**, 14603-14610.

Moudgil, D. K., Westcott, N., Famulski, J. K., Patel, K., Macdonald, D., Hang, H. and Chan, G. K. (2015). A novel role of farnesylation in targeting a mitotic checkpoint protein, human Spindly, to kinetochores. *J Cell Biol* **208**, 881-96.

Nie, L., Spear, E., Babatz, T. D., Quigley, A., Dong, Y. Y., Chu, A., Rotty, B., Chalk, R., Mukhopadhyay, S. M. M., Burgess-Brown, N. A. et al. (2020). A new paradigm for Prelamin A proteolytic processing by ZMPSTE24: the upstream SY^LL cleavage occurs first and there is no CaaX processing by ZMPSTE24. *bioRxiv* doi:10.1101/2020.05.13.093849 .

Oldenburg, K. R., Vo, K. T., Michaelis, S. and Paddon, C. (1997). Recombination-mediated PCR-directed plasmid construction *in vivo* in yeast. *Nucleic Acids Res* **25**, 451-452.

Onono, F. O., Morgan, M. A., Spielmann, H. P., Andres, D. A., Subramanian, T., Ganser, A. and Reuter, C. W. (2010). A tagging-via-substrate approach to detect the farnesylated proteome using two-dimensional electrophoresis coupled with Western blotting. *Mol Cell Proteomics* **9**, 742-51.

Palsuledesai, C. C., Ochocki, J. D., Markowski, T. W. and Distefano, M. D. (2014). A combination of metabolic labeling and 2D-DIGE analysis in response to a farnesyltransferase inhibitor facilitates the discovery of new prenylated proteins. *Mol Biosyst* **10**, 1094-103.

Plummer, L. J., Hildebrandt, E. R., Porter, S. B., Rogers, V. A., McCracken, J. and Schmidt, W. K. (2006). Mutational analysis of the Ras converting enzyme reveals a requirement for glutamate and histidine residues. *J Biol Chem* **281**, 4596-605.

Pronin, A. V., Narovlyansky, A. N. and Sanin, A. V. (2021). New Approaches to the Prevention and Treatment of Viral Diseases. *Arch Immunol Ther Exp (Warsz)* **69**, 10.

Quigley, A., Dong, Y., Pike, A., Dong, L., Shrestha, L., Berridge, G., Stansfeld, P., Sansom, M., Edwards, A., Bountra, C. et al. (2013). The structural basis of ZMPSTE24-dependent laminopathies. *Science* **339**, 1604-7.

Rashidian, M., Dozier, J. K. and Distefano, M. D. (2013). Enzymatic labeling of proteins: techniques and approaches. *Bioconjug Chem* **24**, 1277-94.

Ravishankar, R., Hildebrandt, E. R., Greenway, G., Asad, N., Gore, S., Dore, T. M. and Schmidt, W. K. (2023). Specific Disruption of Ras2 CAAX Proteolysis Alters Its Localization and Function. *Microbiol Spectr* **11**, e0269222.

Reinicke, A. T., Hutchinson, J. L., Magee, A. I., Mastroeni, P., Trowsdale, J. and Kelly, A. P. (2005). A Salmonella typhimurium effector protein SifA is modified by host cell prenylation and S-acylation machinery. *J Biol Chem* **280**, 14620-7.

Ring, J., Tadic, J., Ristic, S., Poglitsch, M., Bergmann, M., Radic, N., Mossmann, D., Liang, Y., Maglione, M., Jerkovic, A. et al. (2022). The HSP40 chaperone Ydj1 drives amyloid beta 42 toxicity. *EMBO Mol Med* **14**, e13952.

Rockmill, B., Lambie, E. J. and Roeder, G. S. (1991). Spore enrichment. *Methods Enzymol* **194**, 146-9.

Runnebohm, A. M., Richards, K. A., Irelan, C. B., Turk, S. M., Vitali, H. E., Indovina, C. J. and Rubenstein, E. M. (2020). Overlapping function of Hrd1 and Ste24 in translocon quality control provides robust channel surveillance. *J Biol Chem* **295**, 16113-16120.

Schey, G., Hildebrandt, E., Wang, Y., Diwan, S., Passetti, H., Potts, G., Sprague-Getsy, A., Leoni, E., Hougland, J., Beese, L. et al. (2023). Library Screening, In Vivo Confirmation, and Structural and Bioinformatic Analysis of Pentapeptide Sequences as Sub-strates for Protein Farnesyltransferase. *submitted*.

Schey, G. L., Buttery, P. H., Hildebrandt, E. R., Novak, S. X., Schmidt, W. K., Hougland, J. L. and Distefano, M. D. (2021). MALDI-MS Analysis of Peptide Libraries Expands the Scope of Substrates for Farnesyltransferase. *Int J Mol Sci* **22,** 12042.

Shoemaker, D. D., Lashkari, D. A., Morris, D., Mittmann, M. and Davis, R. W. (1996). Quantitative phenotypic analysis of yeast deletion mutants using a highly parallel molecular bar-coding strategy. *Nature Genetics* **14**, 450-6.

Sikorski, R. S. and Hieter, P. (1989). A system of shuttle vectors and yeast host strains designed for efficient manipulation of DNA in *Saccharomyces cerevisiae*. *Genetics* **122**, 19-27.

Soveg, F. W., Schwerk, J., Gokhale, N. S., Cerosaletti, K., Smith, J. R., Pairo-Castineira, E., Kell, A. M., Forero, A., Zaver, S. A., Esser-Nobis, K. et al. (2021). Endomembrane targeting of human OAS1 p46 augments antiviral activity. *eLife* **10,** e71047.

Stein, V., Kubala, M. H., Steen, J., Grimmond, S. M. and Alexandrov, K. (2015). Towards the systematic mapping and engineering of the protein prenylation machinery in Saccharomyces cerevisiae. *PLoS One* **10**, e0120716.

Storck, E. M., Morales-Sanfrutos, J., Serwa, R. A., Panyain, N., Lanyon-Hogg, T., Tolmachova, T., Ventimiglia, L. N., Martin-Serrano, J., Seabra, M. C., Wojciak-

Stothard, B. et al. (2019). Dual chemical probes enable quantitative system-wide analysis of protein prenylation and prenylation dynamics. *Nat Chem* **11**, 552-561.

Strutt, H., Thomas-MacArthur, V. and Strutt, D. (2013). Strabismus promotes recruitment and degradation of farnesylated prickle in Drosophila melanogaster planar polarity specification. *PLoS Genetics* **9**, e1003654.

Suazo, K. F., Hurben, A. K., Liu, K., Xu, F., Thao, P., Sudheer, C., Li, L. and Distefano, M. D. (2018). Metabolic Labeling of Prenylated Proteins Using Alkyne-Modified Isoprenoid Analogues. *Curr Protoc Chem Biol* **10**, e46.

Suazo, K. F., Park, K. Y. and Distefano, M. D. (2021). A Not-So-Ancient Grease History: Click Chemistry and Protein Lipid Modifications. *Chem Rev* **121**, 7178-7248.

Trueblood, C., Ohya, Y. and Rine, J. (1993). Genetic evidence for *in vivo* cross-specificity of the CaaX-box protein prenyltransferases farnesyltransferase and geranylgeranyltransferase-I in *Saccharomyces cerevisiae*. *Mol Cell Biol* **13**, 4260-4275.

Varela, I., Pereira, S., Ugalde, A. P., Navarro, C. L., Suarez, M. F., Cau, P., Cadinanos, J., Osorio, F. G., Foray, N., Cobo, J. et al. (2008). Combined treatment with statins and aminobisphosphonates extends longevity in a mouse model of human premature aging. *Nat Med* **14**, 767-72.

Wang, C., Gale, M., Jr., Keller, B. C., Huang, H., Brown, M. S., Goldstein, J. L. and Ye, J. (2005). Identification of FBL2 as a geranylgeranylated cellular protein required for hepatitis C virus RNA replication. *Mol Cell* **18**, 425-34.

Wang, Y. C., Dozier, J. K., Beese, L. S. and Distefano, M. D. (2014). Rapid analysis of protein farnesyltransferase substrate specificity using peptide libraries and isoprenoid diphosphate analogues. *ACS Chem Biol* **9**, 1726-35.

Whitmore, A., Freeny, D., Sojourner, S. J., Miles, J. S., Graham, W. M. and Flores-Rozas, H. (2020). Evaluation of the Role of Human DNAJAs in the Response to Cytotoxic Chemotherapeutic Agents in a Yeast Model System. *Biomed Res Int* **2020**, 9097638.

Whyte, D. B., Kirschmeier, P., Hockenberry, T. N., Nunez-Oliva, I., James, L., Catino, J. J., Bishop, W. R. and Pai, J. K. (1997). K- and N-Ras are geranylgeranylated in cells treated with farnesyl protein transferase inhibitors. *J Biol Chem* **272**, 14459-64.

Wickenhagen, A., Sugrue, E., Lytras, S., Kuchi, S., Noerenberg, M., Turnbull, M. L., Loney, C., Herder, V., Allan, J., Jarmson, I. et al. (2021). A prenylated dsRNA sensor protects against severe COVID-19. *Science* **374**, eabj3624.

Yardeni, D., Heller, T. and Koh, C. (2022). Chronic hepatitis D-What is changing? *J Viral Hepat* **29**, 240-251.

Zhang, F. L., Diehl, R. E., Kohl, N. E., Gibbs, J. B., Giros, B., Casey, P. J. and Omer, C. A. (1994). cDNA cloning and expression of rat and human protein geranylgeranyltransferase type-I. *J Biol Chem* **269**, 3175-3180.

Zhang, F. L., Kirschmeier, P., Carr, D., James, L., Bond, R. W., Wang, L., Patton, R., Windsor, W. T., Syto, R., Zhang, R. et al. (1997). Characterization of Ha-ras, N-ras, Ki-Ras4A, and Ki-Ras4B as in vitro substrates for farnesyl protein transferase and geranylgeranyl protein transferase type I. *J Biol Chem* **272**, 10232-9.

Tables and Figures

Table 1. *Summary of number of proteins identified in UniProtKB/Swiss-Prot database with C-terminal CaaX sequences and with shorter and longer CaaX sequences.*

Search String	Human	Non-human Eukaryotes	Viruses[a]		Total
Cxxx>	1207	5047	375		**6629**
Cxxxx> (omitted CCxxx>)	941	3582	462		**4985**
Cxx> (omitted CCxx>)	989	4206	269		**5464**
TOTAL	**3137**	**12835**	**1106**		**17078**

Footnotes for Table 1: [a]Bacteriophage sequences were manually subtracted from the search.

Figure 1. Hildebrandt et al.
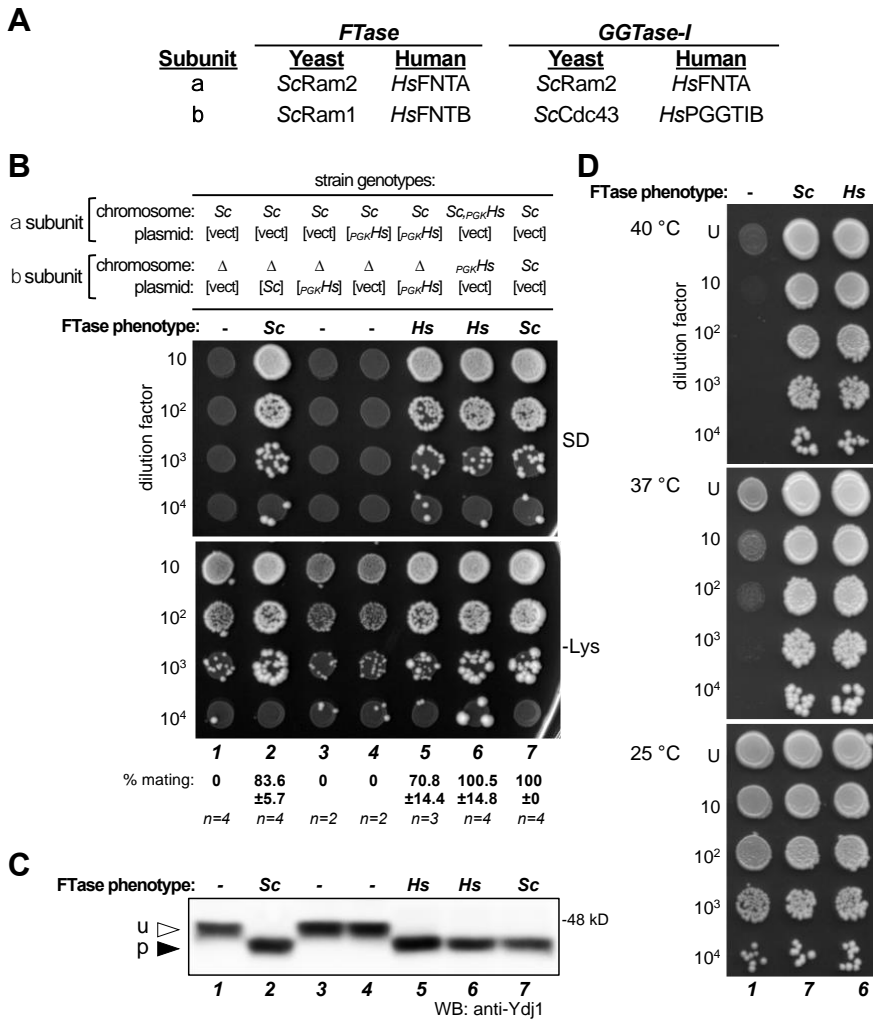
Figure 1. *Interspecies complementation studies of FTase subunits. Hs*FTase and *Sc*FTase subunits are not interchangeable, but co-expression of both α and β subunits of *Hs*FTase can restore FTase activity in the absence of *Sc*FTase. **A**) Relationships between yeast and human prenyltransferase subunits. **B**) The mating assay was used to assess FTase dependent production of **a**-factor. *MAT***a** haploid strains were engineered to express yeast (*Sc*) and/or human FTase α and β subunits (*PGKHs*), where subunits were encoded either on plasmids (indicated by brackets) or from chromosomal loci (no brackets). *MAT***a** strains were mixed with *MAT*α cells (SM1068), mixes subject to 10-fold dilutions, and dilution mixtures spotted onto minimal media (SD) and SC-lysine (-Lys) media. Growth on SD indicates diploid formation, which is a direct indicator of **a**-factor mating pheromone production. Growth on -Lys reflects the input of *MAT***a** cells and reflects both unmated haploid and mated diploid cells; unmated haploid cells (*ram1Δ*) grow less well on -Lys due to the absence of FTase activity. Quantitative mating test results are reported below each lane relative to the WT strain (**7**). Strains used were yWS3276 (**1**), yWS3277 (**2**), yWS3278 (**3**), yWS3408 (**4**), yWS3280 (**5**), yWS3282 (**6**), and yWS3283 (**7**). **C**) Gel-shift analysis of Ydj1 using the same strains described in panel **B**. Total cell lysates were prepared and equivalent protein amounts analyzed by Western blot using anti-Ydj1 antibody. u – unprenylated Ydj1; p – prenylated Ydj1. **D**) Thermotolerance test of the FTase-deficient strain compared to wildtype and humanized FTase strains described in panel **B**. Strains used were yWS3276 (**1**), yWS3282 (**6**), and yWS3283 (**7**).

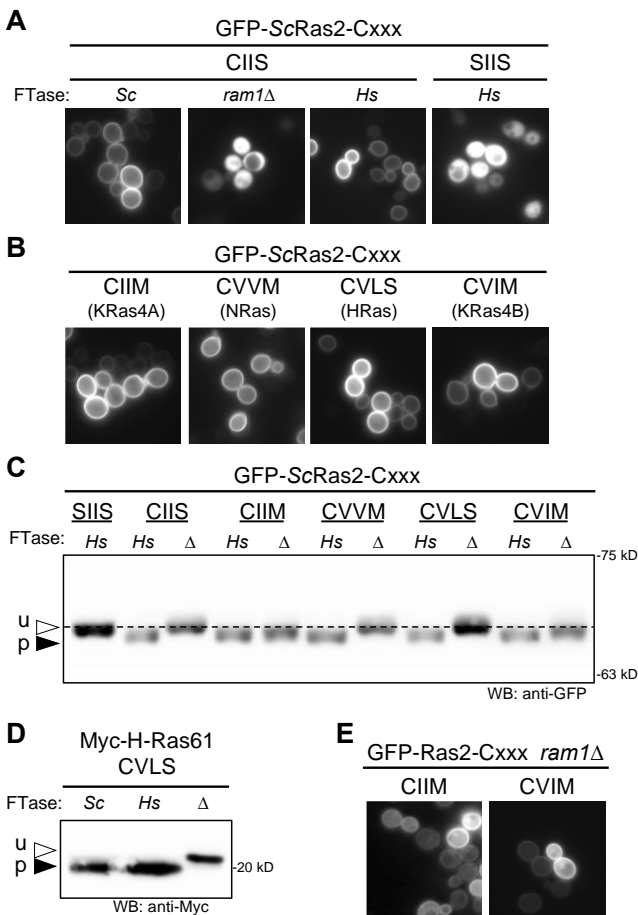**Figure 2.** Hildebrandt et al.

Figure 2. *The humanized FTase strain fully modifies yeast and human Ras CaaX sequences.* GFP-Ras2 was used as a reporter to evaluate CaaX sequences derived from yeast Ras2 (CIIS) and human proteins KRas4A (CIIM), NRas (CVVM), HRas (CVLS), and KRas4B (CVIM). **A**) The localization of GFP-*Sc*Ras2 produced in wildtype (*Sc*), humanized (*H*s), and FTase-deficient (*ram1Δ*) yeast strains was determined by fluorescence microscopy. GFP-*Sc*Ras2-SIIS is a mutant that cannot be prenylated and is cytosolically localized. **B**) The localization of GFP-*Sc*Ras2-CaaX variants encoding human Ras CaaX sequences produced in the humanized FTase strain was determined by fluorescence microscopy. The source of the CaaX sequence is indicated below each specific sequence. **C**) Western blot analysis of GFP-*Sc*Ras2-CaaX variants produced in humanized (*Hs*) or FTase-deficient (Δ) yeast strains. Total cell lysates were prepared, and equivalent protein amounts analyzed by SDS-PAGE and Western blot using anti-GFP antibody. u –unprenylated GFP-*Sc*Ras2; p – prenylated GFP-*Sc*Ras2. The dashed line was aligned with unprenylated GFP-Ras2 to serve as a visual reference. The plasmids used in panels **A-C** were pWS1735 (GFP-*Sc*Ras2), pWS1889 (GFP-*Sc*Ras2-SIIS), pWS1997 (GFP-*Sc*Ras2-CIIM), pWS1998 (GFP-*Sc*Ras2-CVVM), pWS1999 (GFP-*Sc*Ras2-CVLS), and pWS2000 (GFP-*Sc*Ras2-CVIM). pWS1889 encodes a double cysteine to serine mutation; the upstream cysteine is typically palmitoylated but was mutated to avoid creation of a non-canonical length CaaaX sequence. Yeast strains used were BY4741 (wildtype *Sc*FTase), yWS3220 (*Hs*FTase), and yWS3202 (*ram1Δ*). **D**) Myc-HRas61 (p-05547) was produced in wildtype (*Sc*; yWS2544), humanized FTase (*Hs*; yWS3186), or FTase-deficient (Δ; yWS3209) yeast strains. HRas61 is the Q61L oncogenic derivative of human HRas (Adari et al., 1988; Farnsworth et al., 1991). **E**) The localization of GFP-*Sc*Ras2-CaaX variants (CIIM and CVIM) that undergo alternate prenylation by *Sc*GGTase-I in the absence of FTase (i.e., *ram1Δ* strain background).
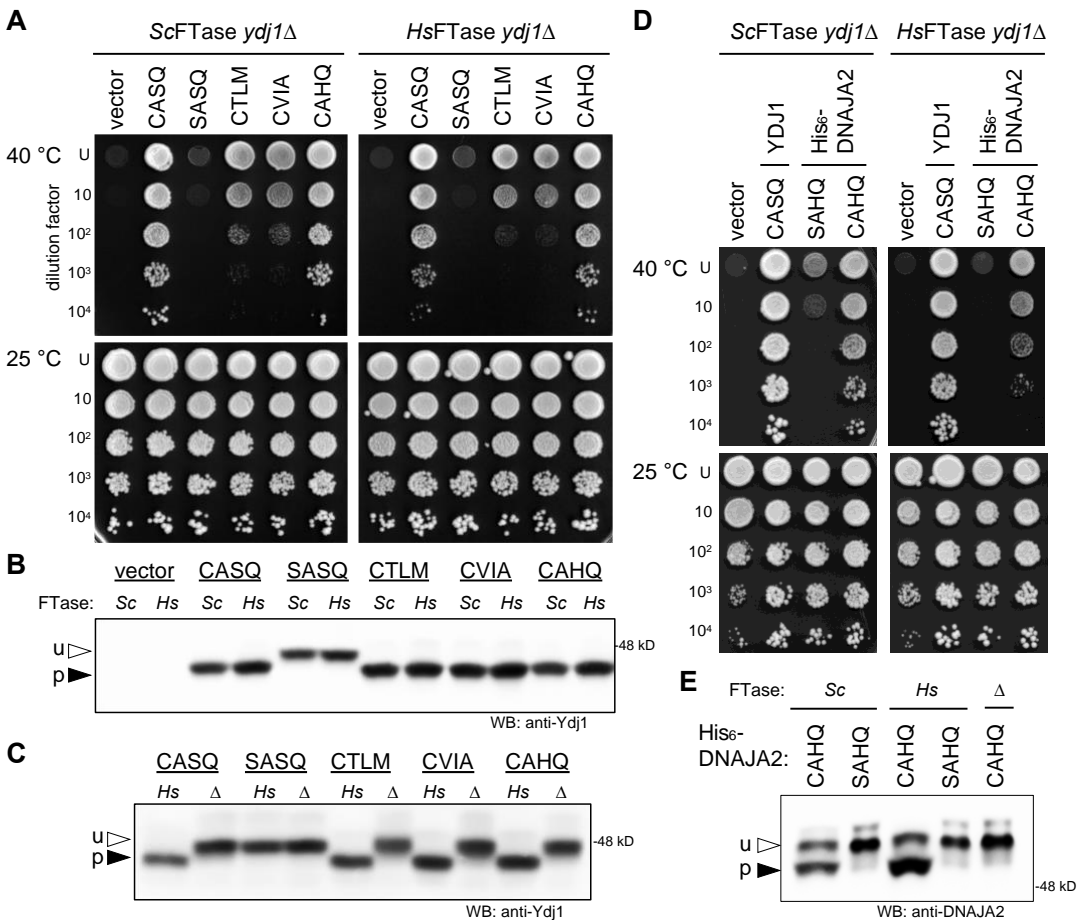
32

Figure 3. Hildebrandt et al.

Figure 3. *The humanized FTase strain modifies HSP40-CaaX variants*. A Ydj1-CaaX reporter was used to evaluate CaaX sequences from yeast HSP40 Ydj1 (CASQ), an unmodifiable sequence (SASQ), yeast Ste18 (CTLM), yeast **a**-factor (CVIA), and human HSP40 DNAJA2 (CAHQ). **A**) The thermotolerance assay was used to determine prenyl modification of Ydj1. Strains were engineered to express *Sc*FTase (left panels) or *Hs*FTase (right panels) and indicated plasmid-encoded Ydj1-CaaX variants. Strains were cultured to equivalent density, cultures subject to 10-fold dilutions, and dilution mixtures spotted onto rich media (YPD) at either room temperature (RT) or elevated temperature (40 °C). Growth at 40 °C reflects farnesylation of Ydj1. **B**) Gel-shift analysis of Ydj1-CaaX variants. Total cell lysates prepared using the strains described in panel **A** were analyzed by SDS-PAGE and Western blot using anti-Ydj1 antibody. u – unprenylated Ydj1; p – prenylated Ydj1. **C**) Comparison of Ydj1-CaaX variant gel mobilities in the absence (Δ) and presence of *Hs*FTase (*Hs*). **D**) Thermotolerance analysis of strains producing native Ydj1 (CASQ), plasmid-encoded human His$_6$-DNAJA2 (CAHQ), and an unmodifiable sequence (SAHQ). Strains were evaluated as described in panel **A**. **E**) Gel-shift analysis of human His$_6$-DNAJA2 and His$_6$-DNAJA2-SAHQ produced in wildtype (*Sc*), humanized FTase (*Hs*), and FTase-deficient (Δ) yeast strains. Total cell lysates were prepared and analyzed as described in panel **B**. For all panels the strains used were yWS2544 (*Sc*FTase *ydj1Δ*), yWS3186 (*Hs*FTase *ydj1Δ;* see **Supplemental Figure S2B**), and yWS3209 (*ram1Δ ydj1Δ*). Plasmids used were pRS316 (vector), pWS942 (YDJ1), pWS1132 (YDJ1-SASQ), pWS1246 (YDJ1-CTLM), pWS1286 (YDJ1-CVIA), pWS1495 (YDJ1-CAHQ), pWS1424 (His$_6$-DNAJA2), and pWS2256 (His$_6$-DNAJA2-SAHQ).
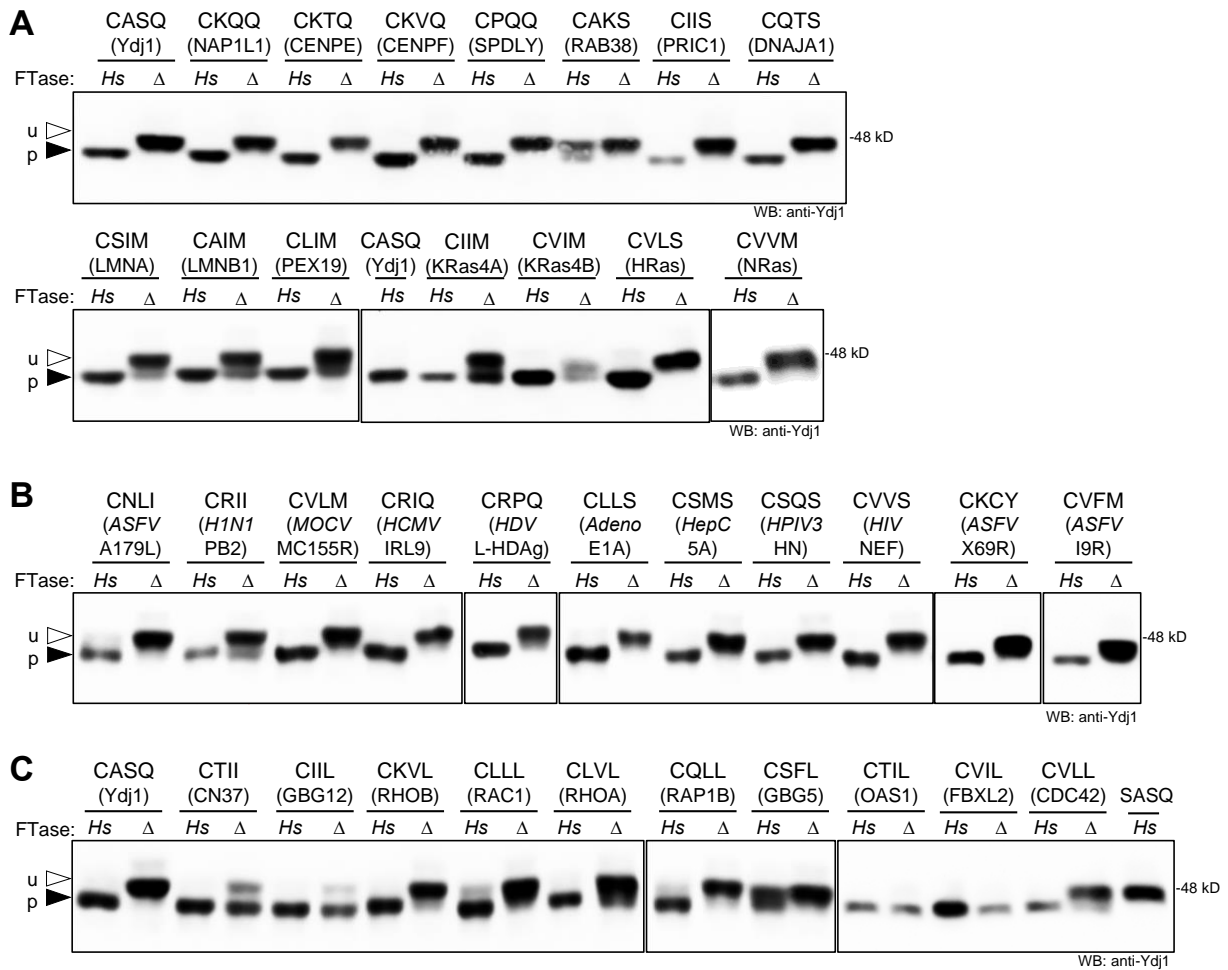
Figure 4. Hildebrandt et al.

Figure 4. *The humanized FTase yeast strain modifies Ydj1-CaaX variants with CaaX sequences occurring in human and viral proteins.* Ydj1-CaaX variants were produced in the *Hs*FTase (*Hs*) and FTase deficient (Δ) strains and evaluated by gel-shift assay as described in **Figure 3B**. The source of the CaaX sequence is indicated below each specific sequence. **A**) Analysis of Ydj1-CaaX variants based on the indicated human proteins. **B**) Analysis of Ydj1-CaaX variants based on mammalian viral proteins. Virus abbreviations are human influenza virus (*H1N1*), Molluscum contagiosum virus (*MOCV*), human cytomegalovirus (*HCMV*), Hepatitis Delta Virus (*HDV*), human adenovirus 1 (*Adeno*), human Hepatitis C virus (*HepC*), human parainfluenza virus 3 (*HPIV3*), Human immunodeficiency virus 1 (*HIV*), and African swine fever virus (*ASFV*). **C**) Analysis of Ydj1 with CaaL/I sequences based on the indicated human proteins. Strains used were yWS3186 (*Hs*) and yWS3209 (Δ). Plasmids used are listed in **Supplemental Table S3**. See **Supplemental Table S1** for gel quantification.
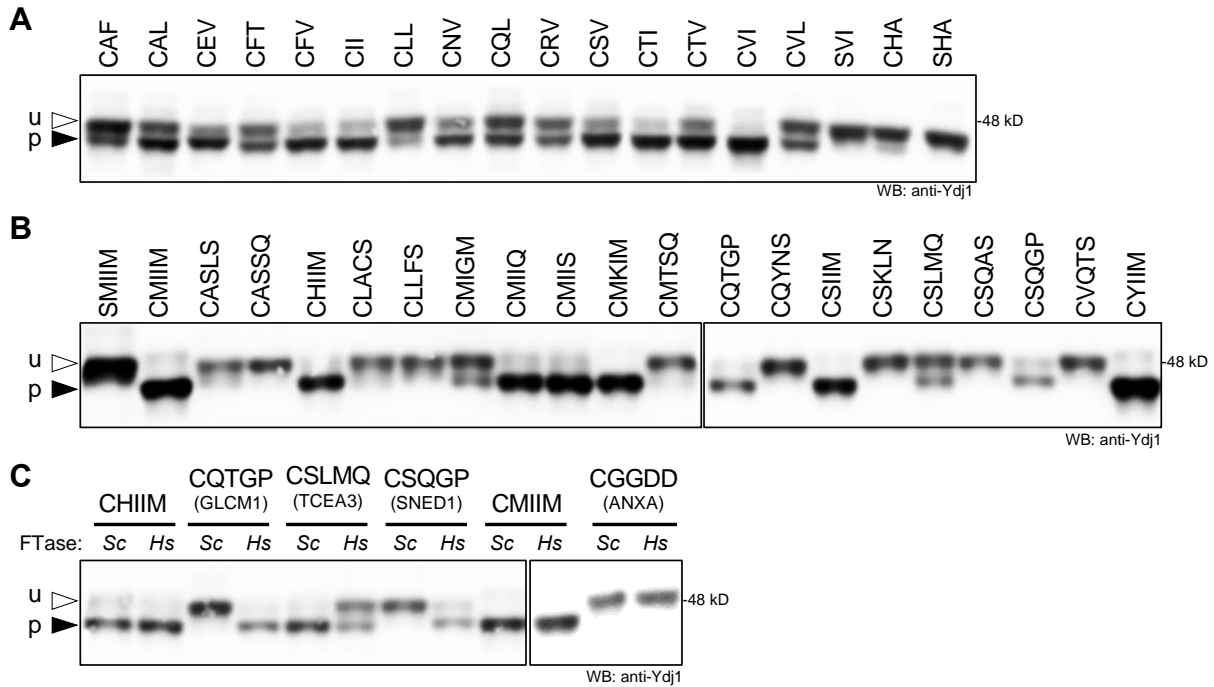
34

Figure 5. Hildebrandt et al.

Figure 5. *The humanized FTase yeast strain modifies certain non-canonical length sequences.* Ydj1-CaaX variants with **A**) shorter CaX and **B**) longer CaaaX sequences were produced in the humanized FTase strain and evaluated by gel-shift assay as described in **Figure 3**. u – unprenylated Ydj1; p – prenylated Ydj1. **C**) Comparison of Ydj1-CaaaX variant gel mobilities in the presence of *Sc*FTase (*Sc*) and *Hs*FTase (*Hs*). The source of the CaaaX sequence is indicated below each specific sequence. Total cell lysates were prepared and evaluated as described in **Figure 3B**. Strains used were yWS3186 (*Hs*FTase ydj1Δ) and yWS2544 (*Sc*FTase *ydj1Δ*). Plasmids used are listed in **Supplemental Table S3**. See **Supplemental Table S1** for gel quantification.
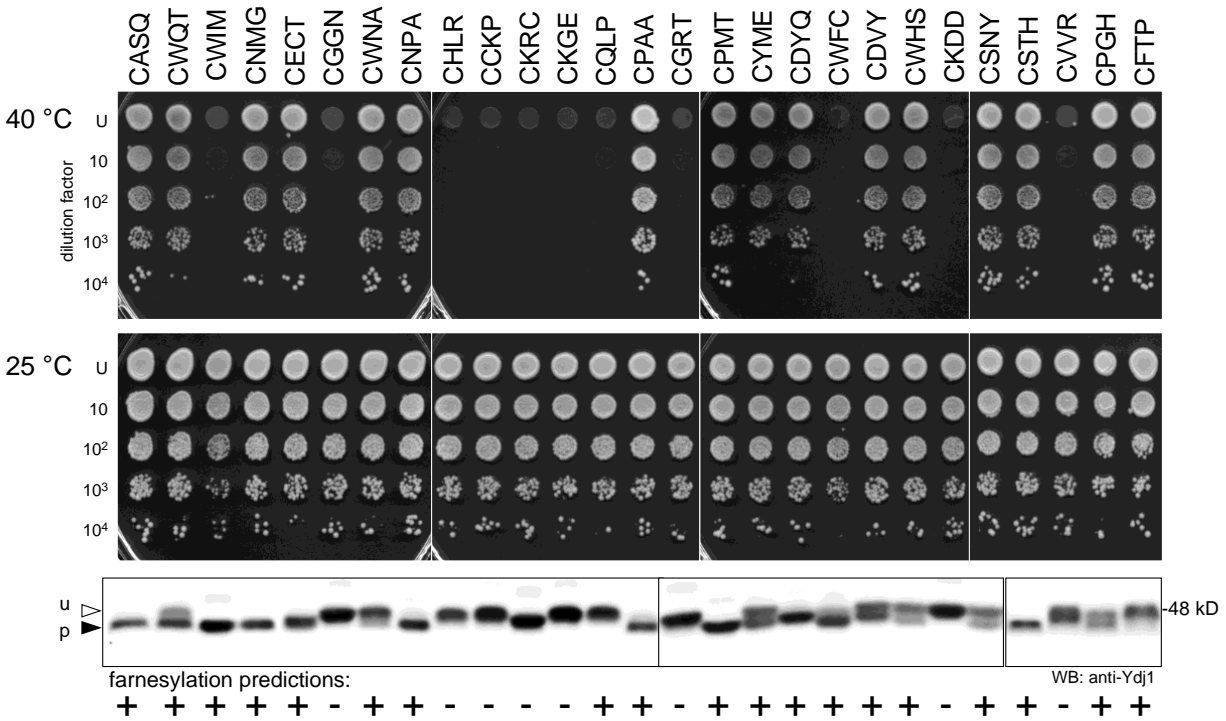
Figure 6. Hildebrandt et al.

Figure 6. *Miniscreen using the humanized FTase strain for identifying prenylatable CaaX sequences.* The humanized FTase yeast strain (yWS3186) was transformed with a plasmid library encoding all 8000 Ydj1-CaaX variants. Plasmids were recovered and sequenced from a randomly selected population of thermotolerant and temperature-sensitive colonies. The plasmids were individually retransformed into yWS3186 and resultant strains evaluated by thermotolerance (upper panels), and gel-shift assays (lower panel) as described in **Figure 3**. Predictions for the farnesylation of each sequence by *Sc*FTase are indicated at the bottom of the figure. Predictions were derived using Heat Map prediction scores reported in Kim et al (Kim et al., 2023); HM score >3 predicts farnesylation, HM score <3 predicts not farnesylated. See **Supplemental Table S1** for gel quantification.

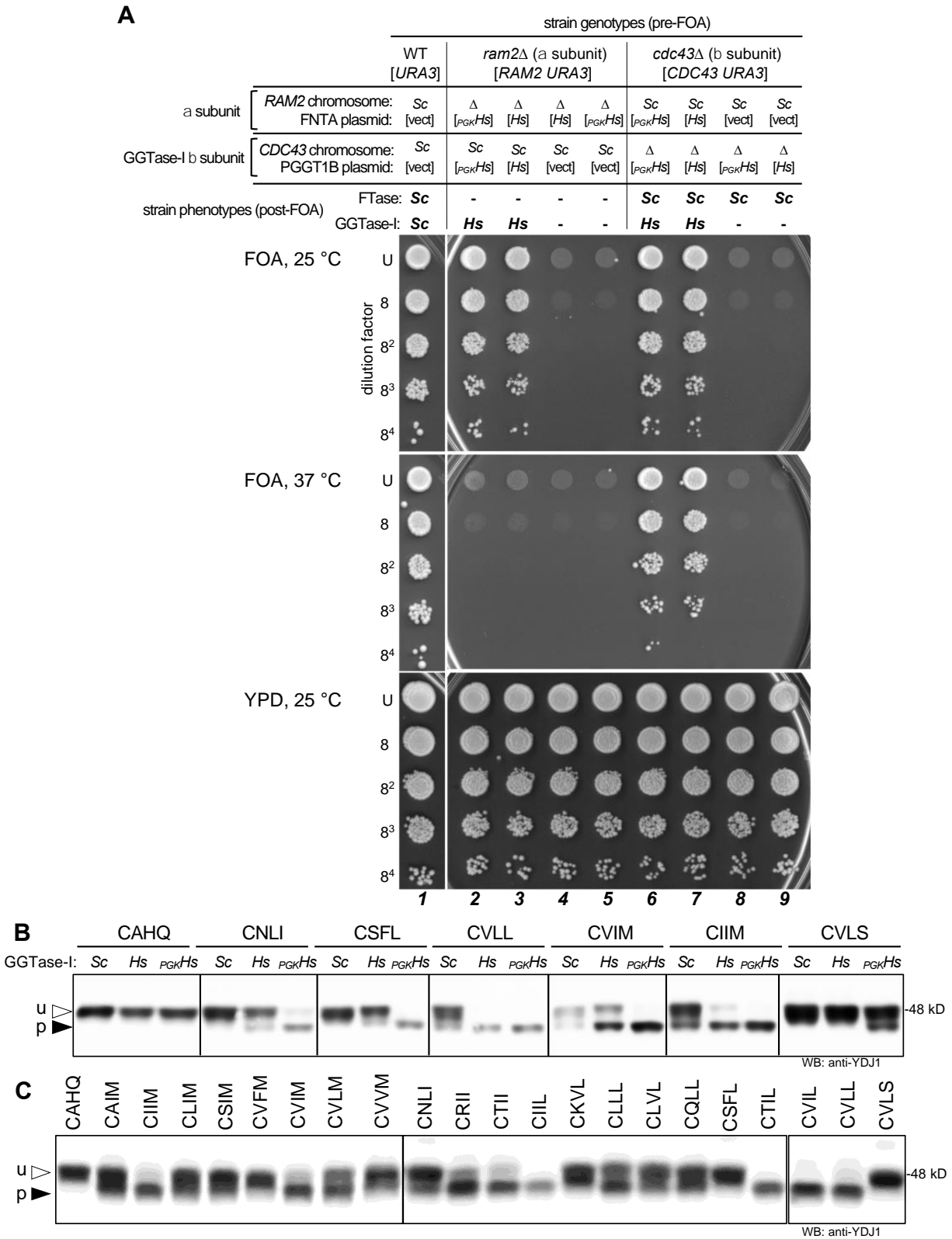**Figure 7.** Hildebrandt et al.

Figure 7. *Interspecies complementation studies of GGTase-I subunits*. *Hs*GGTase-I and *Sc*GGTase-I subunits are not interchangeable, but co-expression of both α and β subunits of *Hs*GGTase-I in yeast can restore GGTase-I activity in the absence of *Sc*GGTase-I. **A**) Viability assay to assess GGTase-I-dependent growth. The yeast genetic backgrounds have only one of the naturally encoded *Sc*GGTase-I subunits encoded on the chromosome, with the presence (*Sc*) and absence (Δ) of the specific subunit indicated above the panel. Because GGTase-I activity is essential for yeast viability, the other subunit is plasmid-encoded. The strains also contain plasmid(s) encoding *Hs*GGTase-I FNTA and/or PGGT1B subunits (indicated by brackets) driven by either the orthologous yeast gene promoter (*Hs*) or the *PGK1* promoter (*$_{PGK}$Hs*). Select strains were also transformed with empty vectors ([vect]) so that all strains had the same selectable markers. The pre-FOA strain genotypes are indicated at the top of the panel. Strains were cultured to the same density, serially diluted, and the dilution series mixtures spotted onto YPD and 5FOA media. Growth on YPD media provides an assessment for the quality of the serial dilutions. 5FOA media counter selects for the *URA3* gene and effectively eliminates the *URA3*-marked plasmid, resulting in the post-FOA phenotypes indicated at the top of the panel. Growth on 5FOA at 25 °C indicates the presence of functional GGTase-I (**2**, **3**, **6** and **7**). Growth on 5FOA at 37 °C is also dependent on functional FTase, which requires α and FTase β subunits of the same species (**6** and **7**). Strains used were yWS3481 (**1**), yWS3388 (**2**), yWS3414 (**3**), yWS3639 (**4**), yWS3287 (**5**), yWS3387 (**6**), yWS3413 (**7**), yWS3285 (**8**), and yWS3638 (**9**). **B)** Gel-shift analysis of Ydj1-CaaX variants produced in yeast expressing *Sc*GGTase-I (*Sc*) or plasmid-encoded *Hs*GGTase-I (*Hs* or *$_{PGK}$Hs*). Total cell lysates were prepared and analyzed as described in **Figure 3B**. Strains used were yWS3209 (*Sc),* yWS3451 (*Hs*), and yWS3169 (*$_{PGK1}$Hs*). **C)** The humanized GGTase-I strain allows prenylation of Ydj1-CaaM/I/L variants taken from human proteins. The expression of GGTase-I subunits in this strain was driven from the orthologous yeast gene promoters to better match the natural *in vivo* activity of yeast GGTase-I. Total cell lysates were prepared and analyzed as described in **Figure 3B**. The strain used was yWS3451. The plasmids in used in this figure are listed in **Supplemental Table S3**. See **Supplemental Table S1** for gel quantification.

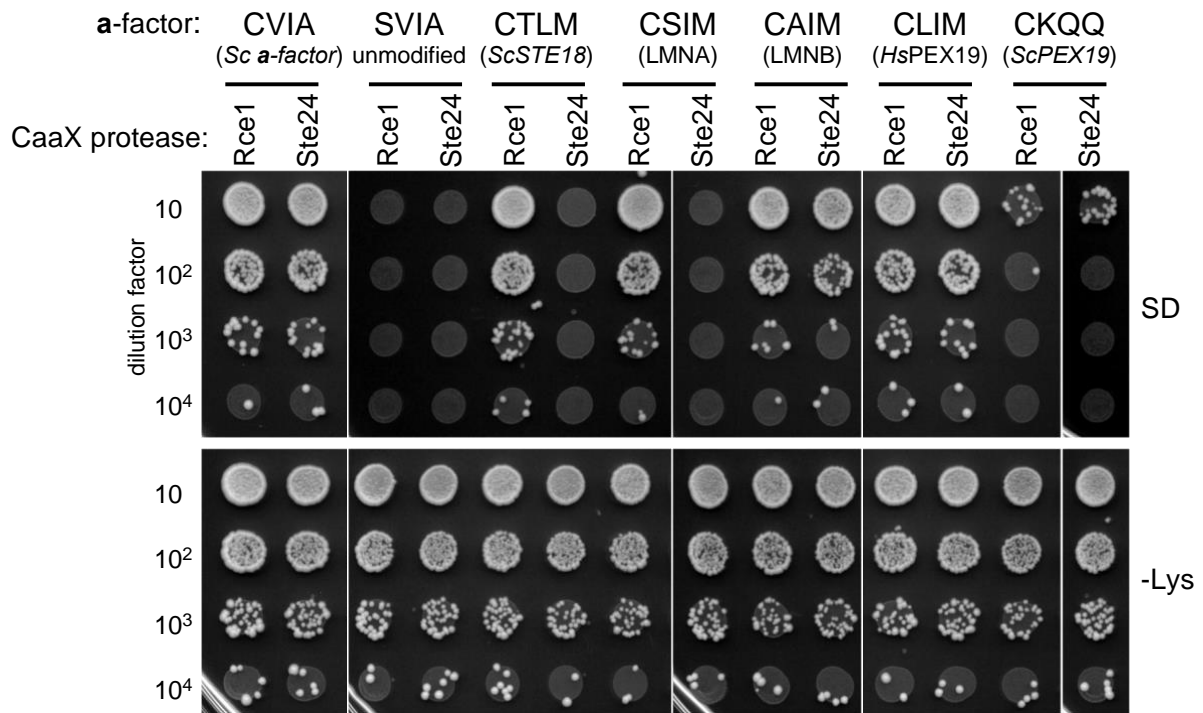**Figure 8.** Hildebrandt et al.

Figure 8. *Prenylation studies can be coupled with CaaX proteolysis studies to better understand CaaX PTMs.* The mating assay was performed as described in **Figure 1B** using *MAT*a strains that carry plasmid-encoded **a**-factor-CaaX variants and plasmid-encoded *Hs*RCE1 (Rce1) or ZMPSTE24 (Ste24) CaaX proteases. The source of the CaaX sequence is indicated below each specific sequence. The strain background for this experiment lacks endogenous **a**-factor (*MFA1* and *MFA2*) and yeast CaaX protease genes (yWS164; *MAT*a *mfa1Δ mfa2Δ rce1Δ ste24Δ*). *MAT*a strains were mixed with *MAT*α cells (SM1068), mixes subject to 10-fold dilutions, and dilution mixtures spotted onto minimal media (SD) and SC-lysine (-Lys) media. Growth on SD indicates diploid formation, which is a direct indicator of **a**-factor mating pheromone production. Growth on –Lys reflects the input of *MAT*a cells. Plasmids are listed in **Supplemental Table S3**.